

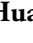



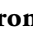




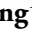
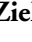





Evolution and classification of hornworts: new insights from the first plastome-based phylogeny

Hao Xu¹ , Chao Shen¹ , Wen-Zhuan Huang² , D. Christine Cargill³ , Juan Carlos Villarreal A.⁴ ,
Sahut Chantanaorrapint⁵ , Chatchaba Promma⁵ , Yu-Mei Wei⁶ , Boon Chuan Ho^{7,8} ,
Dietmar Quandt⁹ , Tao Peng¹⁰ , You-Liang Xiang¹⁰ , H.Rudi Zielman¹¹ , Vadim A. Bakalin¹² ,
Lei Shu^{1,13}  and Rui-Liang Zhu^{1,13,14} 

¹Bryology Laboratory, School of Life Sciences, East China Normal University, Shanghai, 200241, China; ²College of Life and Environmental Sciences, Hangzhou Normal University, Hangzhou, 311121, China; ³Australian National Herbarium, Centre for Australian National Biodiversity Research (a joint venture between the Parks Australia and CSIRO), GPO Box 1700, Canberra, ACT, 2601, Australia; ⁴Département de Biologie, Université Laval, G1V 0A6, Québec City, QC, Canada; ⁵Division of Biological Science, Faculty of Science, Prince of Songkla University, Hat Yai, Songkhla, 90110, Thailand; ⁶Guangxi Key Laboratory of Plant Conservation and Restoration Ecology in Karst Terrain, Guangxi Institute of Botany, Guangxi Zhuang Autonomous Region and Chinese Academy of Sciences, 85 Yanshan Street, Guilin, Guangxi, 541006, China; ⁷Singapore Botanic Gardens, National Parks Board, 1 Cluny Road, Singapore, 259569, Singapore; ⁸Department of Biological Sciences, National University of Singapore, 14 Science Drive 4, Singapore, 117543, Singapore; ⁹Bonn Institute of Organismic Biology (BIOB), University of Bonn, 53115, Bonn, Germany; ¹⁰School of Life Science, Guizhou Normal University, Huaxi District, Guiyang, Guizhou, 550025, China; ¹¹Wooldrikshoekweg 104, 7535 DD, Enschede, the Netherlands; ¹²Laboratory of Cryptogamic Biota, Botanical Garden-Institute of the Far Eastern Branch of the Russian Academy of Sciences, Makovskogo Street 142, Vladivostok, 690024, Russia; ¹³Institute of Advanced Agricultural Science and Technology, East China Normal University, Shanghai, 200241, China; ¹⁴Shanghai Institute of Eco-Chongming (SIEC), Shanghai, 200062, China

Summary

Authors for correspondence:
Rui-Liang Zhu
Email: rlzhu@bio.ecnu.edu.cn

Lei Shu
Email: lshu@bio.ecnu.edu.cn

Received: 8 July 2025
Accepted: 30 September 2025

New Phytologist (2025)
doi: 10.1111/nph.70672

Key words: Cretaceous–Paleogene extinction event, divergence time, new combination, new species, plastid genome, RNA editing.

- Hornworts (Anthocerotophyta) represent a key lineage for understanding fundamental questions in land plant evolution, but their phylogeny and evolutionary history are still not well understood, primarily due to limited genomic resources and insufficient taxon sampling.
- We conducted comparative genomic analyses of 106 hornwort plastid genomes, including 91 newly generated ones. RNA editing sites were identified by integrating transcriptome data and in silico predictions. Additionally, a new method inspired by marker–capture strategies was proposed to estimate the total number of U-to-C editing sites.
- Hornwort plastomes are larger than those of liverworts and mosses, with rare gene loss or pseudogenization. Both C-to-U and U-to-C RNA editing occur across all lineages except *Leiosporoceros*. Diversification rate analyses indicate a major shift between c. 100 and 50 million years ago, possibly linked to the Cretaceous–Paleogene extinction event. Both morphological and molecular evidence support the merging of *Folioceros* into *Anthoceros*, and the recognition of two new species in the small genera *Paraphymatoceros* and *Phymatoceros*, respectively.
- This study presents the first large-scale plastome phylogeny of hornworts, introduces a DNA-only method for estimating the number of U-to-C RNA editing sites, and updates the classification. These results contribute broadly to our understanding of early land plant evolution.

Introduction

Bryophytes, comprising hornworts (Anthocerotophyta), liverworts (Marchantiophyta), and mosses (Bryophyta), represent an ancient lineage of land plants that diverged as the sister clade to all vascular plants c. 500 million years ago (Mya) (Donoghue *et al.*, 2021; Bowman, 2022; Shen *et al.*, 2025). Among these, hornworts represent the least diverse phylum, with 223 currently accepted species (Villarreal *et al.*, 2010b; Brinda & Atwood, 2025). This group exhibits several unique biological features,

including a unique sporophyte architecture, cyanobacterial symbiosis, and a pyrenoid-based carbon-concentrating mechanism (Smith & Griffiths, 1996; Li *et al.*, 2020; Robison *et al.*, 2025). These distinctive characteristics, coupled with their sister position to liverworts and mosses, render hornworts particularly crucial for reconstructing the evolutionary history of land plants. Since the publication of the first phylogenetic classification of hornworts based on *trnL–trnF* and *rbcL* markers (Stech *et al.*, 2003; Duff *et al.*, 2004), substantial progress has been made in elucidating the classification, phylogeny, and evolutionary history of this

group. Key advancements include insights into pyrenoid evolution (Villarreal & Renner, 2012), resolution of deep-level systematic relationships (Cargill *et al.*, 2005; Duff *et al.*, 2007; Peñaloza-Bojacá *et al.*, 2025), evolution of key traits such as sexual systems, antheridial morphology, plastids and stomata (Renzaglia *et al.*, 2009; Hanson *et al.*, 2014; Villarreal & Renner, 2012; Frangedakis *et al.*, 2021a), and understanding of biogeographic patterns and diversification processes (Villarreal *et al.*, 2015b). Furthermore, significant taxonomic revisions have been achieved through the reclassification of existing genera and the description of new taxa, primarily based on analyses of multiple molecular markers (Villarreal *et al.*, 2010a; Peng & Zhu, 2014; Zhang *et al.*, 2018; Cargill & Palsson, 2021). A significant milestone in hornwort research was achieved with the publication of high-quality genomes for 11 hornwort species (Li *et al.*, 2020; Zhang *et al.*, 2020; Schafran *et al.*, 2025). Among these, *Anthoceros agrestis* Paton has emerged as a proper model organism for studying fundamental aspects of land plant biology, physiology, and evolution (Gerke *et al.*, 2020; Frangedakis *et al.*, 2021a, 2021b; Robison *et al.*, 2025; Ruaud *et al.*, 2025). Despite these advancements, the evolutionary trajectory and phylogenetic relationships within hornworts remain contentious, primarily because of insufficient taxonomic sampling across key lineages, reliance on molecular markers with limited phylogenetic resolution, and methodological inconsistencies arising from divergent analytical approaches. Several critical aspects of hornwort evolution remain unresolved, including: the evolutionary dynamics of plastid genomes; the distribution and phylogenetic implications of RNA editing events; temporal and spatial patterns of lineage diversification; and the systematic positions of taxonomically challenging genera, such as *Leiosporoceros*. Furthermore, the monophyly of several morphologically distinct genera, including *Folioceros*, continues to be a subject of ongoing debate (Hasegawa, 1988; Cargill *et al.*, 2022; Bechteler *et al.*, 2023; Li *et al.*, 2024).

In the 'genomic era', plastomes have emerged as pivotal tools in plant phylogenetics and taxonomic revisions because of their highly informative content and greater stability (Daniell *et al.*, 2016; Tonti-Filippini *et al.*, 2017; Li *et al.*, 2019; Xiang *et al.*, 2022). Additionally, in phylogenetic studies, considering the rarity of saturated substitutions in plastid genomes, comprehensive sampling provides certain advantages for studying ancient lineages (e.g. Pollock *et al.*, 2002; Hedtke *et al.*, 2006; Costa *et al.*, 2016). So far, tens of thousands of plastid genomes have been published (Turudić *et al.*, 2023). Plastid genomes are undoubtedly suitable data sources for phylogenetic studies in hornworts, as hornworts have extremely rare cases of polyploidy and exhibit few hybridization events (Proskauer, 1957; Kuta *et al.*, 1990; Fritsch, 1991). Although the first plastid genome of hornworts was reported as early as 2003 (Kugita *et al.*, 2003), our understanding of hornwort phylogeny and evolutionary history based on plastome data remains very limited.

In particular, RNA editing in plastid genomes represents an important but understudied aspect of hornwort molecular evolution. It plays a crucial role in modulating plant phenotype and growth by preserving evolutionarily conserved amino acids

(Takenaka *et al.*, 2013; Sloan, 2017; Small *et al.*, 2020; Knoop, 2023). C-to-U RNA editing is present in the plastid genomes of almost all land plants except for most marchantioid liverworts (Wolf *et al.*, 2004; Rüdinger *et al.*, 2008; Shen *et al.*, 2024), while U-to-C editing is found only in hornworts, ferns, and lycophytes (Knie *et al.*, 2016; Fauskee *et al.*, 2025). Compared with C-to-U editing, which has been studied extensively in terms of evolutionary history and mechanisms, U-to-C editing is still not well studied (Kugita *et al.*, 2003). Studies have found that *Anthoceros agrestis* exhibits 636 C-to-U and 913 U-to-C edits, both of which represent remarkably high levels (Gerke *et al.*, 2020). However, in *Leiosporoceros dussii* (Steph.) Hässel, only 109 C-to-U editing sites have been identified within its plastid genome, and no U-to-C editing has been discovered (Duff & Moore, 2005; Villarreal *et al.*, 2018). This suggests that RNA editing distribution may vary significantly among different taxa, indicating taxonomic specificity. Investigating the editing evolutionary pattern of all genera can help understand the RNA editing evolution and facilitate a better selection of study subjects in future investigations.

In this study, we conducted comprehensive sequencing of plastid genomes representing all known genera of hornworts on a global scale. Our research objectives were fivefold: (1) to establish a robust phylogenetic framework for hornworts based on plastome data and to provide more precise divergence time estimates compared with previous studies using a limited set of molecular markers; (2) to investigate and characterize the evolutionary history of hornwort plastid genomes; (3) to elucidate the distribution patterns of C-to-U and U-to-C RNA editing across all hornwort genera; (4) to examine potential evidence for ancient extinction events in hornworts; and (5) to propose a revised classification for hornworts.

Materials and Methods

Taxon sampling

A global-scale sampling initiative was carried out to account for the extensive molecular diversity observed in hornworts. To address the existing gaps in previous research, special emphasis was placed on wide sampling from southwestern China and the Himalayas, which is one of the hotspots of biodiversity, especially of hornworts in the world (Myers *et al.*, 2000; Villarreal *et al.*, 2010a) because very limited sampling from these regions was included in previous phylogenetic studies (Villarreal *et al.*, 2015b). A total of 106 plastid genomes of hornworts, including 91 newly generated ones, were included in this study, representing all recently recognized genera and 59 species (Supporting Information Table S1). Six published plastomes from liverworts, mosses, and vascular plants were selected as outgroups (Table S1). *Mesoceros*, a small genus with two species disjunction between China and Papua New Guinea, was not included in our analyses owing to its questionable genetic status. Both *Mesoceros* species were described based on a mixed collection of *Phaeoceros* and *Anthoceros* (Cargill & Villarreal, pers. comm). All newly sequenced plastid genomes have been deposited in the GenBase database within the National Genomics Data Center (NGDC).

To investigate the status and relationships of the two new species of *Paraphymatoceros* and *Phymatoceros* identified in our study, we selected the *rps4*, *rbcl*, *matK*, and *nad5* sequences of the broadest taxon sampling thus far (Tables S2, S3).

DNA extraction and sequencing

The tissues of gametophytes and/or sporophytes were selected under a dissecting microscope, cleaned with distilled water to avoid potential contamination from other organisms, and dried in silica gel. The total genomic DNA was extracted, following the modified CTAB method (Allen *et al.*, 2006) with Plant DNAzol Kit (Thermo Fisher Scientific, Waltham, MA, USA) after the plant materials were washed with 0.1 mol l^{-1} Hepes buffer to remove polysaccharides. A DNA library with an insert size of 800 bp was constructed using the Illumina TruSeq™ DNA PCR-free library preparation kit (Illumina, CA, USA). The library was then sequenced on an Illumina HiSeq 2000 platform (PE150) at BGI (Shenzhen, China), generating *c.* 3 Gb of raw data per sample (Chen *et al.*, 2018).

Plastome assembly and annotation

GETORGANELLE v.1.7.5 was employed to assemble the plastid genome (Jin *et al.*, 2020). To address the presence of long simple sequence repeats with a minimum length of 115 bp repeats, an extended k-mer size ($k = 127$) was used, which allowed capturing and resolving these repetitive regions. The resulting assembly was annotated using the GeSeq website (Tillich *et al.*, 2017) and subsequently was manually inspected and revised in the GENEIOUS PRIME v.11.0.4 software (Kearse *et al.*, 2012). Aberrant positions of start and stop codons sometimes suggest the possibility of C-to-U and U-to-C RNA editing events, respectively. C-to-U editing can convert ACG to AUG in mRNA, or convert CAA, CAG, CGA to UAA, UAG, UGA, thereby generating a start or stop codon, manifesting as an aberrant start or stop codon in the DNA sequence (Hoch *et al.*, 1991; Kudla *et al.*, 1992). Similarly, U-to-C RNA editing can result in aberrant stop codons in the DNA sequence by converting UAA, UAG, UGA to CAA, CAG, CGA in mRNA (Knie *et al.*, 2016). Considering this situation, we used the abnormal start codons and stop codons to preliminarily predict the abundance of RNA editing. To determine the correct start and stop codon positions, we selected the plastid genome of *Leiosporoceros*, which lacks U-to-C RNA editing, as a reference (Villarreal *et al.*, 2018). The presumed C-to-U and U-to-C RNA editing were annotated using the ReFernment R package (Robison & Wolf, 2019). The number of predicted RNA editing sites is denoted as n_1 in the section ‘Estimation of the total number of RNA editing sites’.

RNA extraction and sequencing

Total RNA was isolated using the TRIzol reagent (Thermo Fisher Scientific, Waltham, MA, USA). To remove ribosomal RNAs (rRNAs), the RiboMinus Plant Kit for RNA-Seq

(Thermo Fisher Scientific) was employed. The resulting rRNA-depleted RNA was then used for the construction of a stranded RNA-Seq library using the TruSeq mRNA Library Kit. Paired-end sequencing ($2 \times 150 \text{ bp}$) was performed on the Illumina HiSeq Xten platform at Novogene (Beijing, China).

Determination of RNA editing event

RNA reads were first aligned to the plastomes using TOPHAT2 (Kim *et al.*, 2013) with default parameters. The resulting BAM files were then sorted using SAMTOOLS (Li *et al.*, 2009). These sorted alignment files, along with their corresponding genome sequences, were loaded into GENEIOUS PRIME (Kearse *et al.*, 2012). To detect RNA editing events in protein-coding genes (PCGs), the ‘Find Variations’ tool in GENEIOUS PRIME was applied with the following thresholds: minimum coverage = 3, minimum variant frequency = 0.1, maximum variant P -values = 10^{-6} , and minimum strand-bias P -value = 10^{-5} when exceeding 65% bias. The number of detected RNA editing sites is denoted as n_2 in the section ‘Estimation of the total number of RNA editing sites’.

Estimation of the total number of RNA editing sites

Because of sequencing biases and differential gene expression levels, only parts of PCGs are typically covered in transcriptome data, making it nearly impossible to identify all RNA editing sites through transcriptome-based detection alone. Given that RNA editing site prediction and editing site identification from transcriptome data are two statistically independent processes, the Lincoln–Peterson estimator (Lincoln, 1930) – commonly used in capture-recapture models – was applied to estimate the actual total number of RNA editing sites. The estimation formula is:

$$\hat{N} = \frac{n_1 \times n_2}{m}$$

n_1 : the number of predicted RNA editing sites, n_2 : the number of RNA editing sites identified from transcriptome data, m : the number of overlapping sites between prediction and transcriptome identification, \hat{N} : the estimated total number of RNA editing sites.

To examine the correlation between the estimated total number of RNA editing sites \hat{N} and the number of predicted sites n_1 , we performed a linear regression analysis with n_1 as the independent variable and \hat{N} as the dependent variable. The fitted model is as follows:

$$\hat{N} = an_1 + b$$

We also calculated the coefficient of determination (R^2) to evaluate the goodness of fit and performed significance testing on the regression model by computing the corresponding p -values to determine whether the observed relationship is statistically meaningful.

Phylogenetic analyses

We employed maximum likelihood (ML) and Bayesian inference (BI) analyses to infer the phylogenetic relationships. Given the potential issue of substitution saturation in noncoding regions, we focused on a selected set of 80 common PCGs. Certain PCGs that were either missing or pseudogenized in some samples (*cysT*, *rpl2*, and *rps14*), genes duplicated in the inverted repeat (IR) regions of some samples (*ndhB*, *rps7*, and *rps12*), and two genes that were excessively long and could potentially produce unreliable phylogenetic inference during alignment (*ycf1* and *ycf2*) were excluded from the analysis. The initial alignments of individual genes were generated using MAFFT v.7.505 (Katoh & Standley, 2013) and subsequently adjusted in GENEIOUS PRIME.

The best nucleotide and amino acid substitution models were determined using MODELFINDER (Kalyaanamoorthy *et al.*, 2017). Based on the Akaike information criterion (AIC), Bayesian information criterion (BIC), and the corrected Akaike information criterion (AICc), the GTR + F + R3 model for nucleotides and the HIVw + F + R4 model for amino acids were selected, respectively. IQ-TREE v.2.2.2 was used for ML phylogenetic reconstruction (Nguyen *et al.*, 2015). The BI was performed using MRBAYES 3.2.7 (Ronquist *et al.*, 2012). Two independent runs, each with four chains, were conducted, each beginning with a random tree and sampling one tree every 1000 generations of 30 000 000 generations. The first 25% of the trees were discarded as burn-in in TREEANNOTATOR v.1.10.4 to ensure stationarity of the log likelihood (Drummond & Rambaut, 2007). For the phylogenetic analyses of *Paraphymatoceros* and *Phymatoceros*, based on the four markers *rps4*, *rbcL*, *matK*, and *nad5*, we employed the same methods to construct both ML and BI trees, respectively.

Molecular clock and diversification rate analysis

We used the Bayesian method to estimate the divergence times of hornworts with MCMCTree in the PAML package (Yang, 2007). The topological structure derived from nucleotide sequences using ML was employed, and nucleotide data of 80 PCGs were used as input. The upper bound age of the root node was set to 515.5 Mya. A total of 30 000 000 Markov chain Monte Carlo (MCMC) chains were run, with samples taken every 1000 iterations. The initial 20% of trees were discarded as burn-in. We selected two highly reliable fossils for calibration. Fossil calibration point: (1) *Notothylites nirulai* Chitaley & Yawale from the Deccan Intertrappean beds of Mohgaonka, India (Maastrichtian, 65–70 Ma; Chitaley & Yawale, 1980) was used to constrain the age of the stem node of *Notothylas* Sull. ex A.Gray and *Phaeoceros* Prosk. (including *Paraphymatoceros* Hässel; Chitaley & Yawale, 1980); (2) The age of *Anthoceros* spore type A from the Baqueró Formation, Argentina (118.56 ± 3.7 Mya; Archangelsky & Villar de Seoane, 1996) was used to constrain the stem node of *Anthoceros* and the rest of the hornworts (Archangelsky & Villar de Seoane, 1996).

Diversification rate analyses were conducted using both time-constant and time-variable algorithms in BAMM v.2.5.0

(Rabosky, 2014). To determine the parameters for lambdaInitPrior, lambdaShiftPrior, and muInitPrior, we first utilized the setBAMMpriors function in the BAMMTOOLS package (Rabosky *et al.*, 2014) in R. A genus-level sampling fraction was compiled, and two independent reversible jump Markov chain Monte Carlo (rjMCMC) runs were conducted for 10 million generations, with sampling performed every 5000 generations. A Poisson rate before 1.0 was used, and the first 25% of the sampled generations were discarded as burn-in. Convergence of the rjMCMC runs was assessed using the CODA package, confirming that the effective sample size of n.shifts exceeded 200. The final results were summarized using the BAMMTOOLS package in R. Sampling fractions used in the BAMM analysis are listed in Table S4.

Results

Plastid genome features and variation of hornworts

The plastid genomes of all sequenced hornwort samples share a typical quadripartite structure similar to the majority of terrestrial plants and are characterized by the presence of four distinct regions: a large single-copy (LSC), a small single-copy (SSC), and two IRs. The plastid genomes of hornworts exhibited a size range from 152 099 to 161 990 bp. The length of the LSC region varied from 103 707 to 114 477 bp, while the SSC region ranged from 21 836 to 22 822 bp, and the IRs ranged from 9361–15 903 bp (Fig. 1; Table S1).

The overall GC (guanine-cytosine) content within the hornwort plastid genomes ranged from 30.9% to 37.4%. The GC content in the LSC, SSC, and IRs displayed ranges of 28.5% to 35.9%, 29.6% to 35.9%, and 41.0% to 48.2%, respectively (Table S1). The GC content of the plastid genome in hornworts varied in a lineage-specific manner. The average percentages for each order are as follows: Anthocerotales (32.48%), Notothyladales (34.49%), Dendrocerotales (34.96%), Phymatocerotales (37.35%), and Leiosporocerotales (30.90%; Table S1).

A comprehensive annotation of the plastid genomes revealed a total of 129–135 unique genes, consisting of 85–90 PCGs, 36–37 transfer RNA genes (tRNAs), and 8 rRNA genes (Table S1). Pseudogenization or gene loss was detected in three genes. Pseudogenization or loss of the *rpl2* gene occurred in eight genera, including *Dendroceros*, *Megaceros*, *Nothoceros*, *Phaeomegaceros*, *Phymatoceros*, *Phaeoceros*, *Paraphymatoceros*, and *Notothylas*. Considering the monophyly of all the abovementioned taxa, this event likely occurred in the most recent common ancestor (MRCA) of Dendrocerotales, Phymatocerotales, and Notothyladales. Pseudogenization or loss of the *rps14* gene in the genera *Notothylas*, *Paraphymatoceros*, and *Phaeoceros* suggested that this event likely occurred in the MRCA of Notothyladales. Additionally, pseudogenization or loss of the *cysT* gene was found only in *Dendroceros* (Fig. S1).

RNA editing in hornworts

By identifying the atypical start and stop codons in PCGs, we predicted a total of 2 245 potential C-to-U editing events and

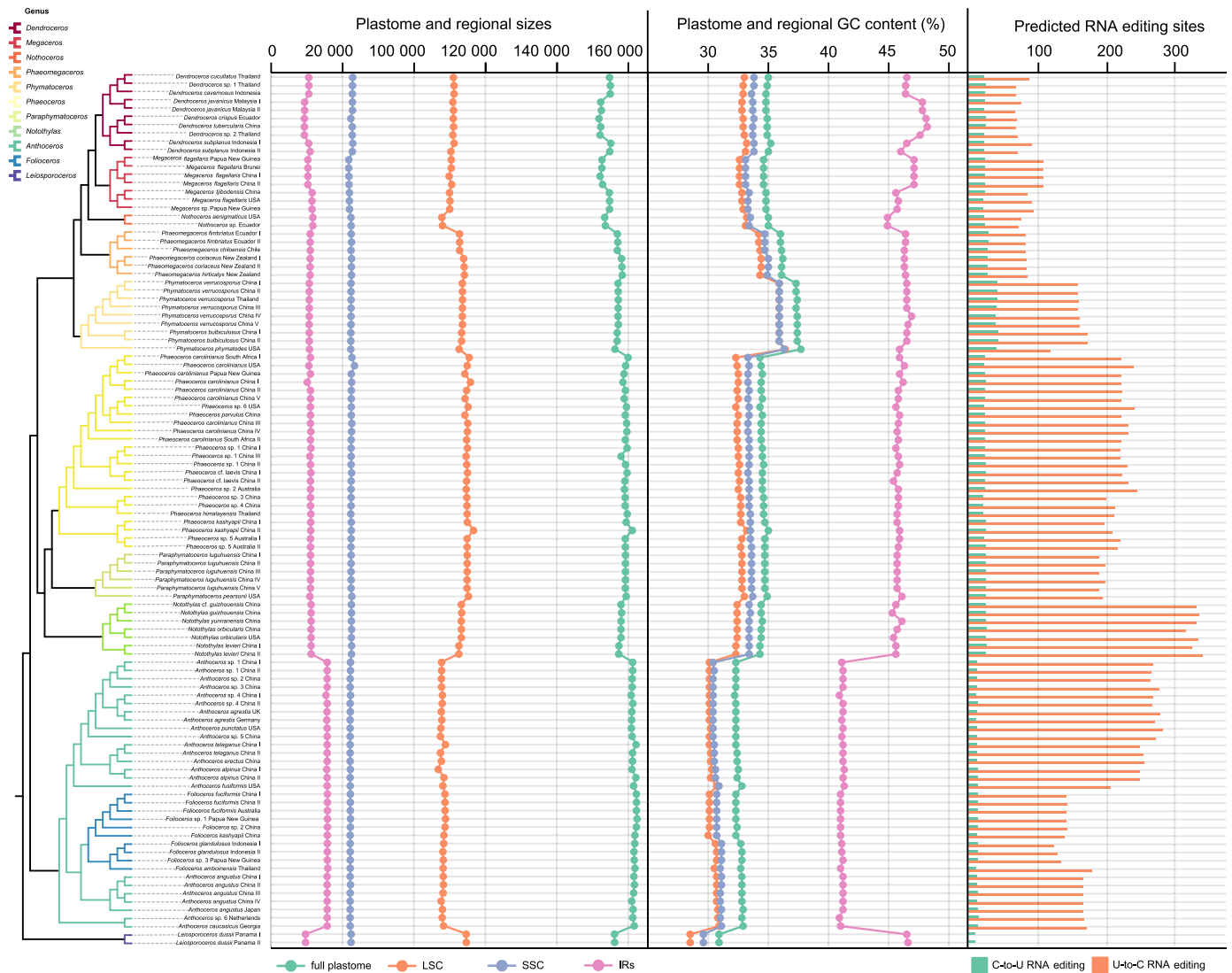


Fig. 1 Comparison of plastome size, GC content, and predicted RNA-editing sites in hornworts. Phylogenetic relationship within hornworts based on nucleotide sequences and maximum likelihood (ML) (far-left), the sizes of the whole plastid genome, large single-copy (LSC), small single-copy (SSC), and inverted repeats (IRs) among all sampled hornworts (left), along with the GC content of each region (middle), the number of C-to-U and U-to-C editing sites predicted by the REFernment R package (far-right).

19 792 U-to-C potential editing events across all samples based solely on DNA sequence (Table S1; Fig. 1).

C-to-U editing was predicted in all samples, with significant differences observed among different species and genera. The lowest number (eight sites) was observed in *Anthoceros agrestis*, and the highest (45 sites) in *Phymatoceros bulbiculosus* (Brot.) Stotler, W.T. Doyle & Crand.Stotl. More U-to-C RNA editing sites were predicted based on abnormal stop codons. The highest number of predicted U-to-C RNA editing sites was found in *Notothylas levieri* Schiffn. ex Steph., with 352 sites predicted, while the lowest number was found in *Dendroceros cavernosus* J.Haseg., with only 71 sites predicted, apart from *Leiosporoceros* where no sites were identified (Table S1).

The RNA editing information derived from five plastid transcriptome samples with good coverage is summarized in Tables S5–S9. The number of sites identified by each method

and their intersections are shown in Table S10; Fig. 2. The results of linear correlation analysis, including the R^2 and P -values for the relationship between the predicted number of editing sites and the estimated total number for each RNA editing type, are shown in Fig. 2. For C-to-U editing, there was no significant linear relationship between the number of predicted sites and the estimated total ($P = 0.3993$, $R^2 = 0.2425$). By contrast, a significant positive correlation was found for U-to-C editing ($P = 0.0091$, $R^2 = 0.9235$).

Phylogenetic relationships within hornworts

The monophyly of nine genera (excluding *Anthoceros* and *Foliosporoceros*) and all higher level relationships showed full support (amino acid-ML-BS (bootstrap support) = 100, DNA-ML-BS = 100, DNA-BPP (Bayesian posterior probability) = 1)

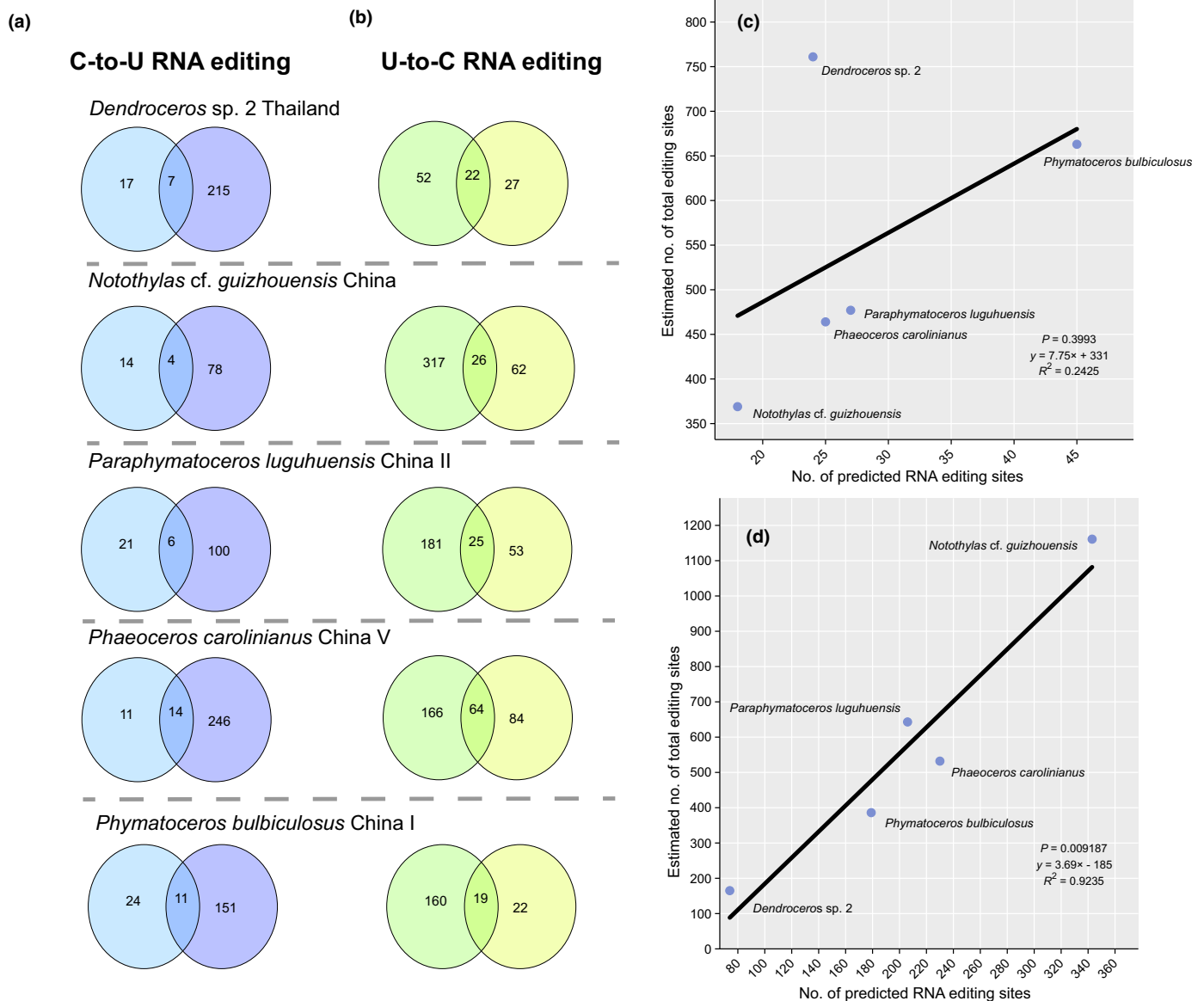


Fig. 2 Number of RNA editing sites in five hornwort samples with transcriptome sequencing data, and correlation between predicted and estimated total numbers. (a, b) Venn diagrams summarizing the number of intersections between predicted RNA editing sites based on DNA sequences (the left circle of each Venn diagram) and the experimentally identified RNA editing sites based on DNA and RNA sequences (the right circle of each Venn diagram). (c, d) The correlation between the estimated total number of RNA editing sites and the number of predicted editing sites. (a, c) C-to-U RNA editing; (b, d) U-to-C RNA editing.

(Figs 3, S2, S3). *Leiosporoceros*, the only genus of Leiosporocerotales, was resolved as sister to all other hornworts with full support (amino acid-ML-BS = 100, DNA-ML-BS = 100, DNA-BPP = 1). Subsequently, Anthocerotales, Notothyladales, Phymatocerotales, and Dendrocerotales diverged in that order, each with full support for monophyly (amino acid-ML-BS = 100, DNA-ML-BS = 100, DNA-BPP = 1). Anthocerotales includes *Anthoceros* and *Folioceros*. *Anthoceros* is paraphyletic in the DNA tree but monophyletic in the amino acid tree (ML-BS = 100), and *Folioceros* is monophyletic in the DNA tree (ML-BS = 100, BPP = 1) but paraphyletic in the amino acid tree. In *Notothyladales*, three genera (*Notothylas*, *Paraphymatoceros*, and

Phaeoceros) are all strongly supported as monophyletic, with the genera branching successively (amino acid-ML-BS = 100, DNA-ML-BS = 100, DNA-BPP = 1). The monotypic *Phymatocerotales* is monophyletic (amino acid-ML-BS = 100, DNA-ML-BS = 100, DNA-BPP = 1). In *Dendrocerotales*, four genera (*Phaeomegaceros*, *Nothoceros*, *Megaceros*, and *Dendroceros*) are monophyletic with successive divergence (amino acid-ML-BS = 100, DNA-ML-BS = 100, DNA-BPP = 1; Figs 3, S2, S3).

We used the DNA-based ML tree as a reference to explore the impact of different tree construction methods on the phylogeny of hornworts. The DNA-based ML tree and the BI tree were almost identical in terms of topology, branch length, and support

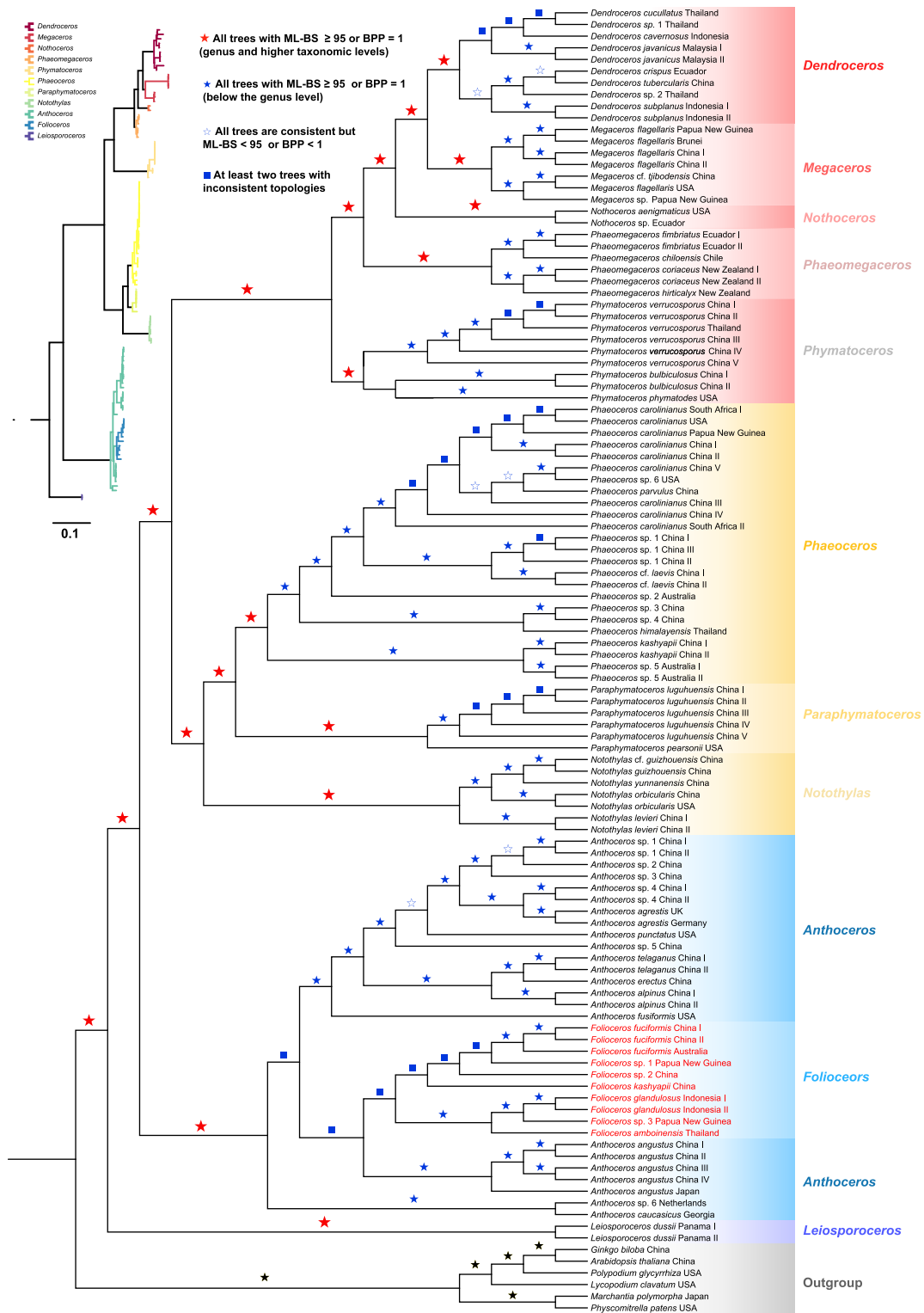


Fig. 3 Joint consensus tree of hornworts inferred from concatenated nucleotide sequences (analyzed using maximum likelihood (ML) and Bayesian inference (BI)) and amino acid sequences (analyzed using ML only). The topological structure presented here is derived from nucleotide sequences using ML. Different symbols on branch nodes represent varying degrees of support and consensus among the three trees. A red solid star indicates nodes at the genus level or higher where the topology is consistent among the three trees with ML-BS = 100 or BPP = 1. A blue solid star represents nodes below the genus level where the topology is consistent among the three trees with ML-BS = 100 or BPP = 1. A blue hollow star represents nodes where the three trees are consistent, but ML-BS or BPP is not 100/1 in one or more trees. A blue square represents nodes where there is conflicting topology among the three trees. The phylogenetic relationships with branch lengths are shown in the top left corner. Since *Folioceros* renders *Anthoceros* paraphyletic, we here synonymize *Folioceros* under *Anthoceros*. All former *Folioceros* samples are highlighted in red on the tree to facilitate inspection of their phylogenetic positions.

values, with only minor variations observed among samples with very close genetic distances, such as the relationship within *Phaeoceros carolinianus* (Michx.) Prosk. By contrast, the amino acid-based ML tree exhibited some differences in topology compared with the DNA-based trees. Notably, the genus *Folioceros* was resolved as paraphyletic, rather than the monophyletic group observed in the DNA-based trees (Figs S2, S3).

Phylogenetic results from the molecular markers (*rbcL*, *rps4*, *matK*, and *nad5*) of *Paraphymatoceros* revealed that the known four species and eight Chinese collections constitute a well-supported clade (ML-BS = 100, SH-aLRT = 100, BPP = 1; Fig. S4). The clade comprises a well-supported group that is proposed as a new species. Similarly, the phylogenetic analyses of four molecular markers showed that the clade comprising five accessions from China and three accessions from Thailand was monophyletic and sister to the remaining *Phymatoceros* species, with high support values (ML-BS = 100, SH-aLRT = 100, BPP = 1; Fig. S5). Consequently, we designated this clade as a new species.

Divergence time and diversification rate analysis

The divergence time estimation based on the MCMCTree reveals that the crown group of hornworts initiated diversification at 512–386 Mya (95% credible interval (CI)). At this node, the monotypic order Leiosporocerotales separated from other hornworts. Subsequently, Anthocerotales diversified at 368–151 Mya (95% CI). The split between Phymatocerotales and Dendrocerotales occurred during the Late Cretaceous (65–78 Mya; 95% CI). At the genus level, within Notothyladales, *Notothylas* diverged *c.* at 47–71 Mya (95% CI), and *Phaeoceros* and *Paraphymatoceros* diverged *c.* at 37–63 Mya (95% CI). In Dendrocerotales, *Phaeomegaceros* diverged first at 45–64 Mya (95% CI), followed by the split of *Nothoceros* at 39–61 Mya (95% CI), and finally the divergence between *Megaceros* and *Dendroceros* at 33–55 Mya (95% CI). For detailed intra-genus divergence times, refer to Fig. 4; Tables S11, S12.

Based on the BAMM analysis, hornworts exhibit a relatively stable background extinction rate, ranging from 0.013–0.019 species million years (Myr)⁻¹. In comparison, the diversification rate during the period before 100 Mya was similar to the background extinction rate, ranging from 0.014 to 0.020 species Myr⁻¹. However, over the subsequent 50 Myr, the diversification rate increased rapidly to 0.042 species Myr⁻¹, leading to a rise in the net diversification rate from 0.001 species Myr⁻¹ to 0.028 species Myr⁻¹. Net diversification rate dynamics of hornwort genera are shown in Fig. 4.

Discussion

Structural features and gene pseudogenization/loss

The plastid genomes of hornworts are notably larger than those of liverworts and mosses. Even the smallest plastid genome reported in hornworts, at 152 099 bp, exceeds the size range of plastid genomes in mosses, which typically range from 120 to

150 kb (Lubna *et al.*, 2024), and in liverworts, where sizes generally fall between 110 and 130 kb (Yu *et al.*, 2019).

The variation in plastid genome size appears to be taxon-specific among land plants. Factors influencing plastid genome size are commonly associated with the number of genes, the length of noncoding regions, and the expansion or contraction of IR regions (Turudić *et al.*, 2023). Through comparative analysis, we found that the larger plastid genome size in hornworts is correlated with the larger size of noncoding regions. Compared with liverworts and mosses, the largest is *Haplomitrium blumei* (Nees) R.M.Schust. (with a total length of 128 728 bp and noncoding regions of 52 053 bp) in liverworts (Yu *et al.*, 2019), and *Takakia lepidozoioides* S.Hatt. & Inoue (Sadamitsu *et al.*, 2021; with a total length of 149 358 bp and noncoding regions of 64 513 bp) in mosses, respectively. The average total size of the genomes in various genera of hornworts is 157 183 bp, with noncoding regions accounting for 70 898 bp (Table S13).

There is little structural variation in the plastid genome of bryophytes. In contrast to angiosperms, which frequently exhibit rearrangements in their plastid genomes, such events are rare among nonvascular plant plastomes; only a few examples of inversions or shifts in the IR boundaries have been documented (Yu *et al.*, 2019; Bell *et al.*, 2020). In mosses, a large inversion of *c.* 71 kb has been identified in the subclass Funariidae (Sugiura *et al.*, 2003; Goffinet *et al.*, 2007). Additionally, a 1-kb inversion associated with gene loss was found in *Aneura mirabilis* (Malmb.) Wickett & Goffinet, a mycoheterotrophic, nonchlorophyllose liverwort known from Europe (Wickett *et al.*, 2008). In all hornwort plastomes examined in the present and earlier studies, only a significant expansion of *c.* 70 kb between the LSC and IRs regions was found in *Anthoceros s. lato* (including *Folioceros*), leading to the duplication of *ndhB*, *rps7*, and *rps12* (Villarreal *et al.*, 2013).

Multiple studies have identified instances of pseudogenization or loss of coding genes for the small and large ribosomal subunits (*rpl*, *rps*) in the organellar genomes of many land plants, with some transfers from plastid and mitochondrial genomes to the nuclear genome (e.g. *rps10* experiencing 26 independent loss events in angiosperms, *rps14* in rice, maize, and wheat; Adams *et al.*, 2000; Adams & Palmer, 2003; Ong & Palmer, 2006). The pseudogenization or loss of *rpl2* and *rps14* in hornwort plastid genomes also suggests potential plastid-to-nucleus or plastid-to-mitochondrion transfers. However, it is worth noting that the pseudogenization of *rpl2* does not occur in several lineages consisting of *Anthoceros s. lato* (including *Folioceros*) and *Leiosporoceros*. The loss of *rpl4* is not common in hornworts, detected only in the Notothyladales lineage, including three genera, *Phaeoceros*, *Paraphymatoceros*, and *Notothylas* (Fig. S1).

The *cysT* gene is one of the nonphotosynthetic genes retained in the plastid genome, and it is responsible for encoding the membrane-associated ATP-binding protein of the sulfate transport system (Lemieux *et al.*, 2000). This gene has been found in most land plants, but it has also undergone numerous independent loss events (Turmel *et al.*, 2005; Sadamitsu *et al.*, 2021). Our results found that *cysT* is pseudogenized or lost in all *Dendroceros* samples, representing the first instance of this gene family missing in hornworts.

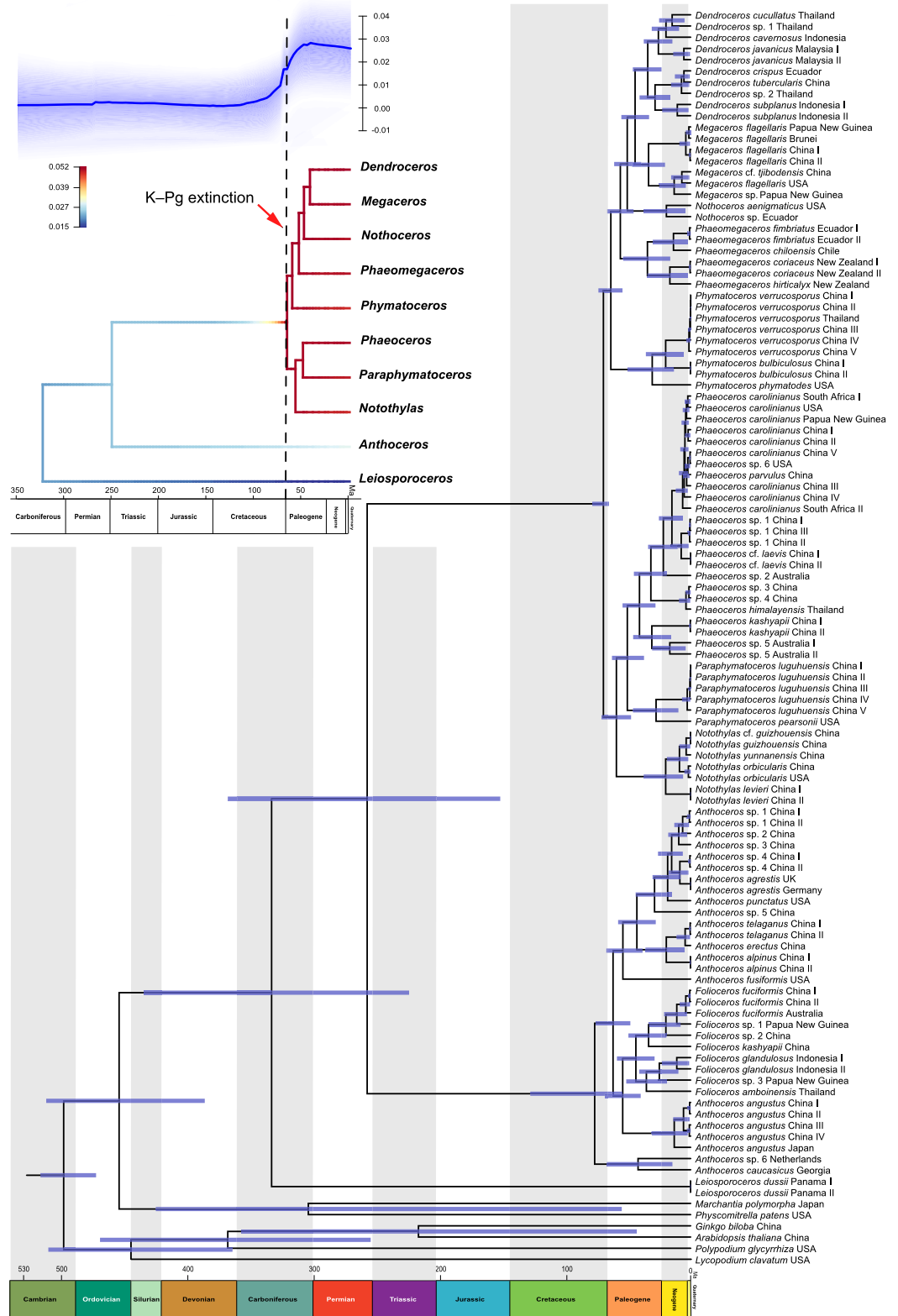


Fig. 4 Divergence time estimation based on MCMCTree using concatenated nucleotide and protein-coding genes (PCGs). Blue bars represent the 95% confidence intervals (CI). The divergence times are detailed in Supporting Information Tables S11, S12, Fig. S7. Net speciation rate dynamics of hornwort genera inferred using BAMM (Bayesian Analysis of Macroevolutionary Mixtures) are displayed in the upper left corner. BAMM analyses incorporated genus-specific sampling fractions (Table S4). The solid blue line represents the mean net diversification rate estimated across all lineages, with the shaded area indicating the 95% credible interval. Branch color denotes estimated net speciation rate (blue: low; red: high). The dashed line indicates the K–Pg boundary (c. 66 million years ago (Mya)), around which a notable rate shift is observed.

C-to-U and U-to-C RNA editing

Recent studies have found instances of loss and regain of RNA editing in certain early land plant lineages, such as the complex thalloid liverworts (Marchantiopsida; Shen *et al.*, 2024), but in

our current sampling, this phenomenon has not been detected in hornworts. All samples investigated in the present study exhibit potential C-to-U editing sites at the start and stop codon positions. C-to-U editing universally present in all genera of hornworts is confirmed here.

U-to-C editing may be considered an ancestral trait inherited from the common ancestor of land plants, gradually diminishing in subsequent evolution (Gerke *et al.*, 2020). The number of U-to-C editing sites varies significantly among various groups of Pteridophytes, which diverged around the same time as hornworts. In some ferns, the number of U-to-C editing sites exceeds that of C-to-U editing (Knie *et al.*, 2016), whereas in the genus *Selaginella* of lycophytes, U-to-C editing is completely absent (Hecht *et al.*, 2011; Oldenkott *et al.*, 2014; Guo *et al.*, 2015). This indicates that U-to-C editing is not conserved throughout evolution in Pteridophyta. Correspondingly, our study found a significant correlation between the number of U-to-C RNA editing sites predicted based on aberrant stop codon insertions and the estimated total number derived from the Lincoln–Peterson method, and the predicted number of U-to-C editing sites varies greatly among different lineages, suggesting that U-to-C RNA editing also has a complex evolutionary history in hornworts.

Another point worth noting is that our study has provided a method to estimate the total number of U-to-C RNA editing solely based on DNA sequences for hornworts. Although the regression model is based on only five representatives, it shows a strong fit to empirical data. The regression equation $y = 3.69x - 185$ yields an estimate of 878 U-to-C editing sites for *A. agrestis*, which closely matches the 913 sites identified from high-quality transcriptomic data (Gerke *et al.*, 2020) – a difference of *c.* 4%. This suggests that the model may be useful for estimating U-to-C RNA editing site abundance in cases where transcriptome data are unavailable, particularly for rare or difficult-to-collect species. However, it should be noted that the predicted number of C-to-U editing sites was not significantly correlated with the estimated actual number, and the regression model cannot be used to infer C-to-U editing abundance.

Molecular phylogeny

In previous studies based on organelle genome DNA markers, the systematic position of *Paraphymatoceros* was uncertain. Duff *et al.* (2007) suggested that *Paraphymatoceros* is sister to *Phaeoceros*, based on *rbcl* analysis. The analysis based on *rbcl* and *nad5*, however, showed that the genus was sister to *Notothylas* (Villarreal & Renner, 2012). Subsequent studies using four molecular markers (*rbcl*, *rps4*, *nad5*, and *matK*) also found *Paraphymatoceros* sister to *Phaeoceros* (Villarreal *et al.*, 2015b). Our study supports Villarreal *et al.*'s (2015b) conclusion. Since our research utilized almost all PCGs on the plastid genome for phylogenetic analysis, this conclusion can be considered definitive for the systematic position of *Paraphymatoceros* at the organelle genome level.

The widespread RNA editing in organelle genomes may influence phylogenetic outcomes (Dong *et al.*, 2023). Duff *et al.* (2007) used two segments of the mitochondrial and plastid genomes, *rbcl* and *nad5*, to construct phylogenetic relationships using two strategies: including/excluding sites modified during RNA editing. In the relationships constructed from the original data, *Leiosporoceros* was placed as sister to all hornwort lineages. However, when RNA editing sites were excluded, this view lost

support. Considering the limitations of the technology at the time, this result may have been due to the scarcity of informative sites. To further assess the effect of bias introduced by using all or only plastome positions modified by the RNA editing machinery, we selected one representative species from each genus and used plastid transcripts to construct a phylogenetic tree, comparing it with the topology of the tree constructed using only plastome DNA sequence data. The tree constructed using RNA sequences showed the same topology compared with DNA sequences at the genus level, and *Leiosporoceros* remained the sister to all other genera of hornworts, with high support values (ML-BS = 100, SH-aLRT = 100, and BPP = 1). This result provides evidence that the presence or absence of RNA editing sites does not significantly affect the deep-level phylogenetic structure in hornworts (Fig. S6).

Most recently, the phylogenetic relationships among hornwort genera have been reconstructed under the multi-species coalescent (MSC) model based on the nuclear gene matrix (Bechteler *et al.*, 2023). The DNA sequences indicated that *Leiosporoceros* and *Anthoceros* formed a single clade, while the amino acid matrix placed *Leiosporoceros* as the sister taxon to the rest of the hornworts. The latest enriched sequencing of hornworts with more comprehensive sampling yielded similar results (Peñaloza-Bojacá *et al.*, 2025). The phylogenetic tree constructed using IQ-TREE indicates that *Leiosporoceros* is sister to all other hornworts, whereas the results from the MSC analysis show that *Leiosporoceros* and the Anthocerotaceae are sister groups (Peñaloza-Bojacá *et al.*, 2025). However, we found that regardless of the data set or methods used, *Leiosporoceros* consistently appears as sister to all remaining hornworts. Considering the long evolutionary history of hornworts, phylogenetic reconstruction based directly on nucleotide sequences might be affected by substitution saturation, introducing noise and impacting the results. By contrast, plastid genes, which evolve more slowly (with substitution rates of only about one-third of the nuclear genome; Wolfe *et al.*, 1987), are less likely to experience substitution saturation (Ravi *et al.*, 2008), resulting in fewer conflicts in deep phylogenetic relationships between the two matrices. Additionally, the latest MSC analysis, based on amino acid sequences from bryophyte transcriptomes – including all extant genera of hornworts and pan-phylum hornwort genomes, also supports *Leiosporoceros* as the sister group to all other hornworts (Schafran *et al.*, 2025; Shen *et al.*, 2025).

Divergence time and mass extinction event

An intriguing question is why hornworts exhibit such a paucity of species diversity compared with mosses and liverworts. Despite their ancient origin, hornworts have a small number of species, with the majority having formed relatively recently. Earlier results based on molecular barcodes (e.g. Villarreal *et al.*, 2015b) indicated that hornworts had few lineages before 55 Mya but may have undergone rapid diversification thereafter. Our dating analyses suggest that this node is somewhat older, being pushed back to *c.* 70 Mya, which brings it closer to the Cretaceous–Paleogene (K–Pg) boundary. Before this boundary, there were only a few

branches of extant hornwort lineages, but after this period, rapid diversification led to the current diversity of over 200 species across *c.* 10 genera. However, it is difficult to believe that such an ancient group would have so few species in the Late Cretaceous after 400 Myr of evolution. Previous views attributed the low species diversity of hornworts to extinction events (Renzaglia *et al.*, 2009). Our finding of a rapid diversification rate shift near the K–Pg boundary suggests a possible postextinction radiation, lending support to this hypothesis.

Although the Cretaceous–Paleogene (K–Pg) mass extinction event seems like a reasonable hypothesis for explaining the current low diversity of hornworts, there are still some open questions to be answered. For example, multiple studies have indicated that mosses and liverworts, also members of the bryophyte divisions, did not exhibit a significant change in species diversification rate at the K–Pg boundary, as inferred from transcriptome and whole-genome data estimates using molecular clocks. The average crown age of orders within mosses and liverworts is *c.* 150.5 Myr, with most family-level MRCA originating during the Jurassic and Cretaceous Periods (Bechteler *et al.*, 2023). Compared with mosses and liverworts, we propose that hornworts may have significant limitations in adapting to harsh environmental conditions, leading to major extinctions. Hornworts have very low morphological variation across the whole group. Therefore, there may be something in their genetic makeup that prevents them from adapting morphologically and physiologically to their new environment, thereby limiting their ability to become highly diverse. Although the K–Pg mass extinction may have affected hornwort diversity, its present low level is more likely attributable to complex adaptive constraints that are still unclear.

Divergence time estimates are highly sensitive to the datasets used, the analytical methods employed, and the fossil calibrations chosen. Nevertheless, the latest study using capture sequencing for divergence time estimates also shows that hornworts underwent significant diversification during the mid-Cretaceous and Paleogene Periods (Peñaloza-Bojacá *et al.*, 2025). The major difference between divergence time estimates based on nuclear genomes and plastid genomes is that the divergence of Notothyladaceae and Dendrocerotaceae began earlier in the former (early Jurassic of the midpoint in the divergence time interval in nuclear data) compared with the latter (late Cretaceous of the midpoint in the divergence time interval in plastid genome data). At the genus level, both studies indicate that the diversification of almost all extant genera began in the early Paleogene.

Taxonomy and nomenclature

Paraphymatoceros, a small genus with only four species, is known only from Chile and the United States in the Americas (Crandall-Stotler *et al.*, 2006; Hässel de Menéndez, 2006; Villarreal *et al.*, 2015a; Söderström *et al.*, 2016), but with one unconfirmed record of *P. pearsonii* (Howe) J.C.Villarreal & Cargill in Taiwan, China (Yang, 1960, as *Anthoceros pearsonii*). Our results reveal that eight collections from southwestern China form a well-supported clade, which is sister to the known four species

(Fig. S4). Morphologically, the Chinese collections are most similar to *Paraphymatoceros proskaueri* (Stotler, Crand.-Stotl. & W.T.Doyle) J.C.Villarreal & Cargill in the similar terminal tubers of thallus, absence of pyrenoid, shorter capsules, rigid columellae, and capsule valves adherent at the apex. The latter, however, differs mainly in dioicous sexuality, a single antheridium per chamber, and abundant lateral tubers in male and female plants (Crandall-Stotler *et al.*, 2006). Thus, both morphological and molecular evidence unambiguously support the recognition of a new species from China: *Paraphymatoceros luguhuensis* as described in the next section (Fig. 5).

Phymatoceros is represented world-wide by only three species (Söderström *et al.*, 2016; Asthana *et al.*, 2023), including *P. binsarensis* A.K.Asthana recently described from Uttarakhand, India, known from only two old collections (Asthana *et al.*, 2023). Unfortunately, suitable samples for DNA extraction were not available. The Indian *P. binsarensis* is well characterized and easily distinguished from the other *Phymatoceros* species by having each facet of the proximal spore surface with a small central hollow, as in *Notothylas yunnanensis* T.Peng & R.L.Zhu, *Paraphymatoceros diadematus* Hässel, *Phaeoceros himalayensis* (Kashyap) Prosk. ex Bapna & G.G.Vyas, and *Phaeomegaceros coriaceus* (Steph.) R.J.Duff (Asthana & Srivastava, 1991; Crandall-Stotler *et al.*, 2006; Peng & Zhu, 2014; Peñaloza-Bojacá *et al.*, 2022). In Asia, besides the common *Phymatoceros bulbiculosus* (Brot.) Stotler, W.T.Doyle & Crand.-Stotl., eight collections from China (Yunnan and Xizang) and Northern Thailand form a well-supported clade (ML-BS = 100, SH-aLRT = 100, BPP = 1) that is sister to other species of *Phymatoceros* (Fig. S5). This interesting lineage is well defined by the strap-shaped thallus usually with stalked tubers on the ventral surface, the large, single antheridium per androecial chamber, randomly arranged jacket cells of the antheridium, the presence of a pyrenoid, short capsule with stomates, one- or two-celled pseudoelaters, and brown spores with a coarsely papillose proximal face without a small central hollow (Fig. 6). Based on morphological characters and unique phylogenetic position in *Phymatoceros*, a new species is proposed.

Folioceros, a genus segregated from *Anthoceros* by Bharadwaj (1971), currently has *c.* 19 accepted species (Söderström *et al.*, 2016). It differs from *Anthoceros* mainly in the strap-shaped thallus, elongated, strongly thick-walled pseudoelaters, and indistinct triradiate mark of the spore (Bharadwaj, 1971; Asthana & Srivastava, 1991; Asthana & Nath, 1999; Cargill *et al.*, 2022). However, the morphological distinction between the two genera is difficult to maintain owing to the morphological overlaps of several key features in the two genera, as shown in Cargill *et al.* (2022). *Folioceros assamicus* D.C.Bharadwaj, the type species of the genus, is poorly known, and the type specimen was deposited in the personal herbarium of the Indian bryologist D.C. Bharadwaj (Bharadwaj, 1971; Asthana & Nath, 1999). The type material, unfortunately, could not be located and may have been lost. Furthermore, known collections of this species kept in the Indian herbaria (e.g. LWU) can actually be assigned to *Folioceros fuciformis* (Mont.) D.C.Bharadwaj (Chantanaorrapint, pers. comm). So far, no suitable collections have been available for molecular analyses. Morphologically, *Folioceros assamicus* is very



Fig. 5 *Paraphymatoceros luguhuensis*. (a) Populations on soil with young sporophytes. (b) Two antheridia. (c) Close-up of gametophyte thalli and sporophytes. (d) Portion of columella. (e) Close-up of plant showing two mature sporophytes. (f) Capsule showing opening line and yellowish spores. (g) Epidermal cells of thallus showing plastids. (h) Transverse section of capsule at middle, only half shown. (i) Transverse section of thallus, only part shown. (j) Capsule epidermis showing a stoma. (k) Pseudoelater. (l–n) Spores, (l–m) proximal view, (n) polar distal view. All from R. L. Zhu *et al.* 20220828-43 (HSNU).

similar to *F. fuciformis* and could even be conspecific. The present phylogenomic analyses using 10 plastomes of *Folioceros* (including *F. fuciformis*) also reveal the clade of *Anthoceros* + *Folioceros* with maximal support values (Figs 3, S2, S3), and *Anthoceros* is polyphyletic, as already shown in Cargill *et al.* (2022), based on

three plastid markers (*rbcL*, *trnK-matK*, and *rps4*). Furthermore, the ML tree based on amino acid sequences shows that *Folioceros* is polyphyletic with high support values (Figs S2, S3). Therefore, based on morphological similarities and overlaps of *Anthoceros* and *Folioceros*, as well as the outcome of the molecular

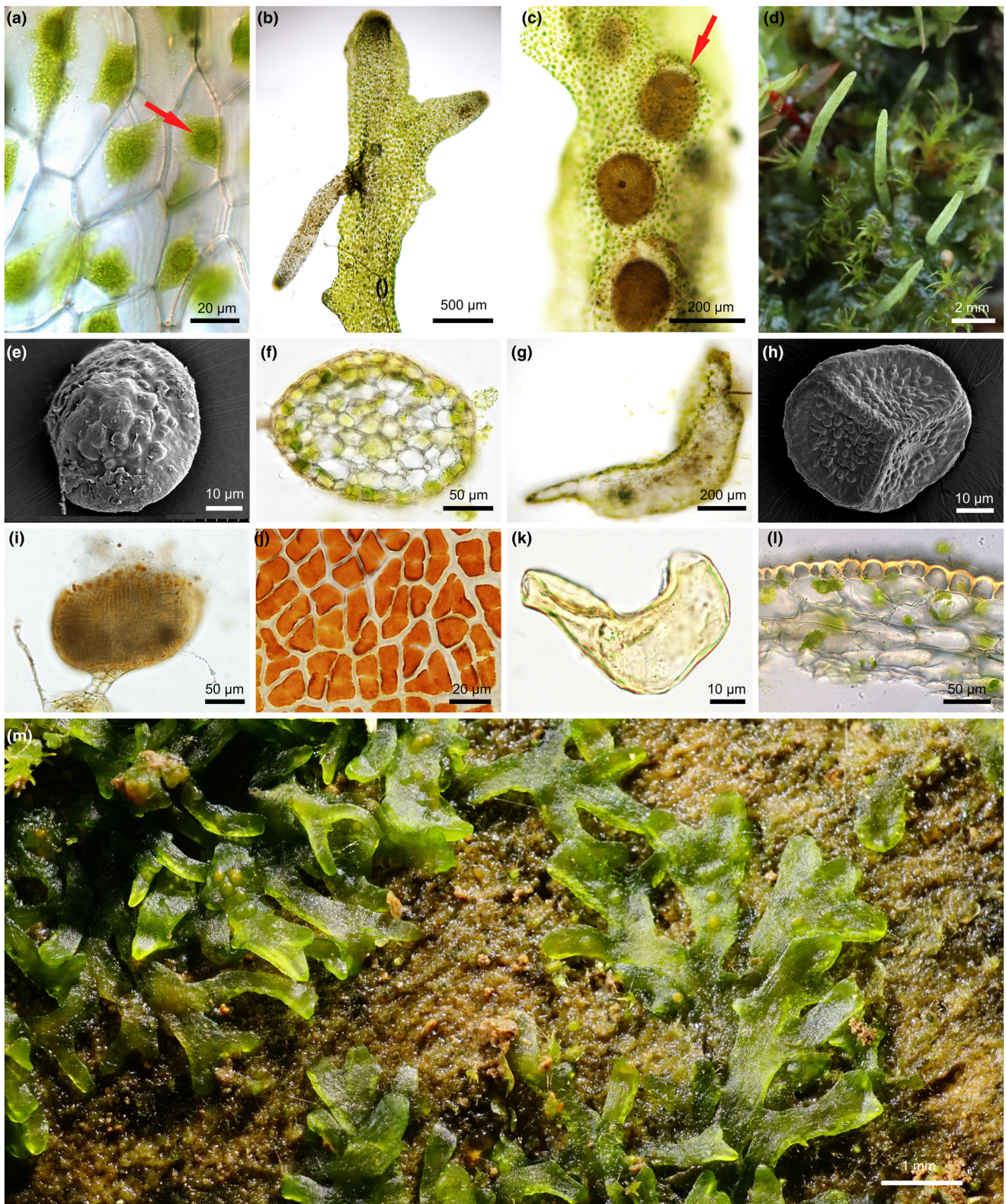


Fig. 6 *Phymatoceros verrucosporus*. (a) Epidermal cells of thallus showing plastid with pyrenoid (indicated by red arrow). (b) Thallus showing a ventral tuber, ventral view. (c) Male plant showing the single antheridium per antheridial chambers (indicated by red arrow). (d) Female plants *in situ* showing sporophytes. (e) Spore, distal face. (f) Transverse section of ventral tuber. (g) Transverse section of thallus. (h) Spore, proximal face. (i) Antheridium showing a short stalk. (j) Median cells of antheridial jacket. (k) Elater. (l) Portion of transverse section of capsule. (m) Male plants *in situ* with antheridial chambers (yellow dots). Images in (d, e, h, k, l) from W. Z. Huang & S. H. Lu 20210906-7A (HSNU), all others from R. L. Zhu *et al.* 20220827-2 (HSNU).

investigation at the plastome level, *Folioceros* is recommended to be subsumed into *Anthoceros*. A nomenclatural change, including seven new combinations, is proposed below.

Taxonomic treatment

***Anthoceros* L.**, Sp. Pl. 2: 1139. 1753. Lectotype designated by Evans (1918): *Anthoceros punctatus* L., Sp. Pl. 1139. 1753.

= *Folioceros* D.C.Bhardwaj, Geophytology 1: 9. 1971. Type: *Folioceros assamicus* D.C.Bhardwaj, Geophytology 1: 10. 1971. **Syn. nov.**

***Anthoceros assamicus* (D.C.Bhardwaj) R.L.Zhu & Cargill, comb. nov.**

Basionym: *Folioceros assamicus* D.C.Bhardwaj, Geophytology 1: 10. 1971.

***Anthoceros indicus* (D.C.Bhardwaj) R.L.Zhu & Cargill, comb. nov.**

Basionym: *Folioceros indicus* D.C.Bhardwaj, Geophytology 8(1): 114. 1978.

***Anthoceros kashyapii* (S.C.Srivast. & A.K.Asthana) R.L.Zhu & Cargill, comb. nov.**

Basionym: *Folioceros kashyapii* S.C.Srivast. & A.K.Asthana, Bryologist 92(2): 219. 1989.

***Anthoceros paliformis* (D.K.Singh) R.L.Zhu & Cargill, comb. nov.**

Basionym: *Folioceros paliformis* D.K.Singh, Bull. Bot. Surv. India 29: 176. 1987[1989].

***Anthoceros physocladus* (D.C.Bhardwaj) R.L.Zhu & Cargill, comb. nov.**

Basionym: *Folioceros physocladus* D.C.Bhardwaj, Geophytology 8(1): 115. 1978.

***Anthoceros satpurensis* (D.C.Bhardwaj & K.P.Srivast.) R.L.Zhu & Cargill, comb. nov.**

Basionym: *Folioceros satpurensis* D.C.Bhardwaj & K.P.Srivast., Geophytology 8(1): 112. 1978.

***Anthoceros udarii* (A.K.Asthana & S.C.Srivast.) R.L.Zhu & Cargill, comb. nov.**

Basionym: *Folioceros udarii* A.K. Asthana & S.C. Srivast., Cryptog. Bryol. Lichénol. 7(2): 151. 1986.

***Paraphymatoceros luguhuensis* R.L.Zhu & Hao Xu, sp. nov. (Fig. 5)**

Type: China, Yunnan, Ninglang Co., Luguhu, Gouzuandong Pass, 27°38'22.03" N, 100°48'41.15" E, 3122 m, on soil, 28 Aug. 2022, *R.L. Zhu, W.Z. Huang & H. Xu 20 220 828–43* (holotype: HSNU! isotype: CANB!).

Diagnosis: Similar to *Paraphymatoceros proskaueri*, but can be distinguished by the monoicous sexuality, 2–4 antheridia per antheridial chamber, capsule dehiscing by two longitudinal slits along two suture lines, and rare occurrence of tubers in fertile plants. A detailed description and key to all species of *Paraphymatoceros* are provided in the Notes S1.

Etymology: The epithet '*luguhuensis*' refers to the locality of the holotype: Luguhu (Lugu Lake).

Habitat and distribution: *Paraphymatoceros luguhuensis* occurs on a soil slope at an elevation of 2600–3130 m on the edge of the coniferous forests. It is known from Binchuan Co., Ninglang Co., and Yulong Co., Yunnan, China. Sporophytes usually mature between late August and early November.

Selected specimens examined (all paratypes): China, Yunnan, Binchuan Co., Jizu Mountain Scenic Spot, 25°57'42.24" N, 100°22'1.14" E, 2657 m, 27 Aug. 2022, *R.L. Zhu et al. 20 220 827–29* (HSNU); Ninglang Co., Luguhu, Gouzuandong Pass, 27°37'55.75" N, 100°49'0.35" E, 3306 m, 21 Nov. 2021, *W.Z. Huang & H. Xu 20 211 119–21* (HSNU); Yulong Co., Laojun Mountain National Geopark, 26°39'13.13" N, 99°49'8.45" E, 2890 m, 2 Sept. 2023, *R.L. Zhu et al. 20230902–77* (HSNU).

***Phymatoceros verrucosporus* R.L.Zhu, Hao Xu & Chantanaorr, sp. nov. (Fig. 6)**

Type: China, Yunnan, Nanjian Co., Wuliangshan National Nature Reserve, Fenghuang Mountain, 24°53'45.68" N, 100°19'55.43" E, 2308 m, on soil, 27 Aug. 2022, *R.L. Zhu, W.Z. Huang, H. Xu 202202827–2* (holotype: HSNU!).

Diagnosis: Similar to *Phymatoceros bulbiculosus*, but can be distinguished by the single antheridium per androecial chamber, coarsely papillose proximal face of the yellow spores, one- or two-celled pseudoelaters, and distal spore face ornamented with mound-like protuberances rather than several irregular ridges.

A detailed description and a key to all species of *Phymatoceros* are provided in the Notes S2.

Etymology: The epithet '*verrucosporus*' refers to the verrucate distal surface of the spore.

Habitat and distribution: *Phymatoceros verrucosporus* occurs on soil on the edge of coniferous forests or on dripping slopes near the summit at altitudes of 2300–3000 m. It is known from northwestern and southwestern China (Xizang and Yunnan) and northern Thailand (Chiang Mai). Sporophytes usually mature between late August and early December.

Selected specimens examined (all paratypes): China, Xizang, Yadong Co., Xiayadong town, 27°24'29.89" N, 88°57'5.55" E, 2889 m, 19 Sept. 2020, *Y.L. Xiang et al. 20200919–46* (HSNU); Yunnan, Nanjian Co., Wuliangshan National Nature Reserve, Fenghuang Mountain, 25 August 2015, *R.L. Zhu et al. 20150825–2* (HSNU). Xundian Co., Black-necked Crane Provincial Nature Reserve, 25°35'12.27" N, 103°1'9.56" E, 2745 m, 6 Sept. 2021, *W.Z. Huang & S.H. Lu 20 210 906–7A* (HSNU); Thailand, Chiang Mai, Doi Inthanon National Park, summit, 18°58.839' N, 98°48.659' E, 2560 m, 20 December 2011, *R.L. Zhu 20 111 220–100* (HSNU).

Updated classification of hornworts

With these new species and new combinations, an updated classification of hornworts with 223 species in 10 genera of five families of four orders is presented (Notes S3).

Conclusion

The first plastome-based phylogenetic study of hornworts reveals that 10 genera of hornworts are well resolved and strongly supported, and that *Leiosporoceros* is identified as the sister to all other hornworts. Phylogenomic analyses show that hornworts have larger plastid genomes than liverworts and mosses due to their relatively large noncoding regions. The structure and gene composition of hornwort plastomes are relatively conservative, with only one significant event of IRs expansion and three pseudogenes identified. The distribution of RNA editing events in different genera or species of hornworts is not even. C-to-U edits are present in all genera of hornworts. Statistical analysis reveals a significant linear correlation between the predicted number of U-to-C editing sites and the total number in hornworts, whereas no such correlation was found for C-to-U editing. Estimations of divergence times and diversification rate analyses suggest that hornwort diversity may have been profoundly affected by the Cretaceous–Paleogene extinction event. *Folioceros* is proposed as a new synonym of *Anthoceros*. The finding of two new species in the small genera *Paraphymatoceros* and *Phymatoceros* suggests that the species diversity of hornworts is probably underestimated.

Acknowledgements

We are grateful to the curators and staff of the herbaria (BR, CANB, E, G, HSNU, IBK, NY, PSU, SZG, and VBG) for loans or donations of specimens. Sincere thanks are extended to S. R. Gradstein for assistance in obtaining the specimens, and we also thank the anonymous reviewers for their constructive and insightful comments. This work was supported by the National Natural Science Foundation of China (nos. 32370218 and 31170190) and East China Normal University (the Research Funds of Happiness Flower ECNU).

Competing interests

None declared.

Author contributions

R-LZ conceived the study. HX collected samples, performed experiments, and analyzed the data. CS and W-ZH analyzed the data. HX, R-LZ, LS, DCC and JCV interpreted the results and wrote the paper. SC, CP, Y-MW, BH, Y-LX, TP, DQ, HRZ and VB collected samples. All authors revised and approved the final manuscript.

ORCID

Vadim A. Bakalin  <https://orcid.org/0000-0001-7897-4305>
D. Christine Cargill  <https://orcid.org/0000-0001-8390-3245>
Sahut Chantanaorrapint  <https://orcid.org/0000-0002-9739-0994>
Boon Chuan Ho  <https://orcid.org/0000-0003-0530-775X>

Wen-Zhuan Huang  <https://orcid.org/0000-0001-5871-5699>
Tao Peng  <https://orcid.org/0000-0002-9255-8751>
Chatchaba Promma  <https://orcid.org/0000-0001-5990-6251>
Dietmar Quandt  <https://orcid.org/0000-0003-4304-6028>
Chao Shen  <https://orcid.org/0000-0002-7553-7457>
Lei Shu  <https://orcid.org/0000-0002-2258-9130>
Juan Carlos Villarreal A.  <https://orcid.org/0000-0002-0770-1446>
Yu-Mei Wei  <https://orcid.org/0000-0002-1845-716X>
You-Liang Xiang  <https://orcid.org/0000-0001-9727-7329>
Hao Xu  <https://orcid.org/0000-0003-2521-1368>
Rui-Liang Zhu  <https://orcid.org/0000-0002-0163-8255>
H.Rudi Zielman  <https://orcid.org/0009-0003-9130-4834>

Data availability

The newly sequenced plastome data have been deposited in the National Genomics Data Center (NGDC), with accession nos.: C_AA110815.1 to C_AA110905.1. All other processed data are available on FigShare (<https://doi.org/10.6084/m9.figshare.29484917.v2>).

References

- Adams KL, Daley DO, Qiu YL, Whelan J, Palmer JD. 2000. Repeated, recent and diverse transfers of a mitochondrial gene to the nucleus in flowering plants. *Nature* 408: 354–357.
- Adams KL, Palmer JD. 2003. Evolution of mitochondrial gene content: gene loss and transfer to the nucleus. *Molecular Phylogenetics and Evolution* 29: 380–395.
- Allen GC, Flores-Vergara MA, Krasynanski S, Kumar S, Thompson WF. 2006. A modified protocol for rapid DNA isolation from plant tissues using cetyltrimethylammonium bromide. *Nature Protocols* 1: 2320–2325.
- Archangel'sky S, Villar de Seoane L. 1996. Estudios palinológicos de la formación Baqueró (Cretácico), provincia de Santa Cruz, Argentina. VII. *Ameghiniana* 33: 307–313.
- Asthana AK, Nath V. 1999. Distributional patterns of the genus *Folioceros* Bharad. in India. *Cryptogamie Bryologie* 20: 257–265.
- Asthana AK, Shukla D, Gupta R. 2023. *Phymatoceros* Stotler *et al.* (Anthocerotophyta) newly recorded from India with a new species, *P. binsarensis*. *Journal of Bryology* 45: 236–242.
- Asthana AK, Srivastava SC. 1991. Indian hornworts. A taxonomic study. *Bryophytorum Bibliotheca* 42: 1–158.
- Bechteler J, Peñaloza-Bojacá G, Bell D, Burleigh JG, McDaniel SF, Davis EC, Sessa EB, Bippus A, Cargill DC, Chantanaorrapint S *et al.* 2023. Comprehensive phylogenomic time tree of bryophytes reveals deep relationships and uncovers gene incongruences in the last 500 million years of diversification. *American Journal of Botany* 110: e16249.
- Bell D, Lin Q, Gerelle WK, Joya S, Chang Y, Taylor ZN, Rothfels CJ, Larsson A, Villarreal JC, Li FW *et al.* 2020. Organellomic data sets confirm a cryptic consensus on (unrooted) land-plant relationships and provide new insights into bryophyte molecular evolution. *American Journal of Botany* 107: 91–115.
- Bharadwaj DC. 1971. On *Folioceros*, a new genus of Anthocerotales. *Geophytology* 1: 6–15.
- Bowman JL. 2022. The origin of a land flora. *Nature Plants* 8: 1352–1369.
- Brinda JC, Atwood JJ. 2025. *The bryophyte nomenclator*. St. Louis: Missouri Botanical Garden, [WWW document] URL <https://www.bryonames.org/>.
- Cargill DC, Chantanaorrapint S, Zhu RL, Asthana AK, Li L, Renzaglia KS, Villarreal JC. 2022. Resolving relationships within the hornwort genus *Anthoceros*. *Bryophyte Diversity and Evolution* 45: 26–43.
- Cargill DC, Palsson R. 2021. Hornworts of Australia: three new *Anthoceros* L. (Anthocerotaceae) species from New South Wales. *Telopea* 24: 325–343.

- Cargill DC, Renzaglia KS, Villarreal JC, Duff RJ. 2005. Generic concepts within hornworts: historical review, contemporary insights and future directions. *Australian Systematic Botany* 18: 7–16.
- Chen Y, Chen YX, Shi CM, Huang ZB, Zhang Y, Li SK, Li Y, Ye J, Yu C, Li Z *et al.* 2018. SOAPnuke: a mapreduce acceleration-supported software for integrated quality control and preprocessing of high-throughput sequencing data. *GigaScience* 7: 1–6.
- Chitale SD, Yawale NR. 1980. On *Notothyrites nirulai* gen. et sp. nov.: a petrified sporogonium from the Deccan-Interrappean beds of Mohgaonkalan M. P. (India). *Botanique* 9: 111–118.
- Costa JF, Lin SM, Macaya EC, Fernández-García C, Verbruggen H. 2016. Chloroplast genomes as a tool to resolve red algal phylogenies: a case study in the Nemaiales. *BMC Evolutionary Biology* 16: 205.
- Crandall-Stotler BJ, Stotler RE, Doyle WT. 2006. On *Anthoceros phymatodes* M. Howe and the hornwort genus *Phymatoceros* Stotler, W. T. Doyle & Crand.-Stotl. (Anthocerotophyta). *Cryptogamie Bryologie* 27: 59–73.
- Daniell H, Lin CS, Yu M, Chang WJ. 2016. Chloroplast genomes: diversity, evolution, and applications in genetic engineering. *Genome Biology* 17: 134.
- Dong SS, Zhou XP, Peng T, Liu Y. 2023. Mitochondrial RNA editing sites affect the phylogenetic reconstruction of gymnosperms. *Plant Diversity* 45: 485–489.
- Donoghue PCJ, Harrison CJ, Paps J, Schneider H. 2021. The evolutionary emergence of land plants. *Current Biology* 31: R1281–R1298.
- Drummond AJ, Rambaut A. 2007. BEAST: Bayesian evolutionary analysis by sampling trees. *BMC Evolutionary Biology* 7: 214.
- Duff RJ, Cargill DC, Villarreal JC, Renzaglia KS. 2004. Phylogenetic relationships of the hornworts based on *rbcL* sequence data: novel relationships and new insights. *Monographs in Systematic Botany from the Missouri Botanical Garden* 98: 41–58.
- Duff RJ, Moore FBG. 2005. Pervasive RNA editing among hornwort *rbcL* transcripts except *Leiosporoceros*. *Journal of Molecular Evolution* 61: 571–578.
- Duff RJ, Villarreal JC, Cargill DC, Renzaglia KS. 2007. Progress and challenges toward developing a phylogeny and classification of the hornworts. *The Bryologist* 110: 214–243.
- Evans AW. 1918. Hepaticae. Liverworts. In: Britton NL, ed. *Flora of Bermuda*. New York, NY, USA: Scribner, 469.
- Fauske BD, Kuo LY, Heath TA, Xie PJ, Pryer KM. 2025. Comparative phylogenetic analyses of RNA editing in fern plastomes suggest possible adaptive innovations. *New Phytologist* 247: 2945–2963.
- Frangedakis E, Shimamura M, Villarreal JC, Li FW, Tomaselli M, Waller M, Sakakibara K, Renzaglia KS, Szóvényi P. 2021a. The hornworts: morphology, evolution and development. *New Phytologist* 229: 735–754.
- Frangedakis E, Waller M, Nishiyama T, Tsukaya H, Xu X, Yue Y, Tjahjedi M, Gunadi A, Van Eck J, Li FW. 2021b. An *Agrobacterium*-mediated stable transformation technique for the hornwort model *Anthoceros agrestis*. *New Phytologist* 232: 1488–1505.
- Fritsch R. 1991. Index to bryophyte chromosome counts. *Bryophytorum Bibliotheca* 40: 1–352.
- Gerke P, Szóvényi P, Neubauer A, Lenz H, Gutmann B, McDowell R, Small I, Schallenberg-Rudinger M, Knoop V. 2020. Towards a plant model for enigmatic U-to-C RNA editing: The organelle genomes, transcriptomes, editomes and candidate RNA editing factors in the hornwort *Anthoceros agrestis*. *New Phytologist* 225: 1974–1992.
- Goffinet B, Wickett NJ, Werner O, Ros RM, Shaw AJ, Cox CJ. 2007. Distribution and phylogenetic significance of the 71-kb inversion in the plastid genome in Funariidae (Bryophyta). *Annals of Botany* 99: 747–753.
- Guo W, Grewe F, Mower JP. 2015. Variable frequency of plastid RNA editing among ferns and repeated loss of uridine-to-cytidine editing from vascular plants. *PLoS ONE* 10: e0117075.
- Hanson DT, Renzaglia K, Villarreal JC. 2014. Diffusion limitation and CO₂ concentrating mechanisms in bryophytes. In: Hanson D, Rice S, eds. *Photosynthesis in bryophytes and early land plants. Advances in photosynthesis and respiration*. Dordrecht, the Netherlands: Springer, 95–111.
- Hasegawa J. 1988. A proposal for a new system of the Anthocerotae, with a revision of the genera. *The Journal of the Hattori Botanical Laboratory* 64: 87–95.
- Hässel de Menéndez GG. 2006. *Paraphymatoceros* Hässel, gen. nov. (Anthocerotophyta). *Phytologia* 88: 208–211.
- Hecht J, Grewe F, Knoop V. 2011. Extreme RNA editing in coding islands and abundant microsatellites in repeat sequences of *Selaginella moellendorffii* mitochondria: the root of frequent plant mtDNA recombination in early tracheophytes. *Genome Biology and Evolution* 3: 344–358.
- Hedtke SM, Townsend TM, Hillis DM. 2006. Resolution of phylogenetic conflict in large data sets by increased taxon sampling. *Systematic Biology* 55: 522–529.
- Hoch B, Maier R, Appel K, Igloi GL, Kössel H. 1991. Editing of a chloroplast mRNA by creation of an initiation codon. *Nature* 353: 178–180.
- Jin JJ, Yu WB, Yang JB, Song Y, dePamphilis CW, Yi TS, Li DZ. 2020. GetOrganelle: a fast and versatile toolkit for accurate *de novo* assembly of organelle genomes. *Genome Biology* 21: 241.
- Kalyaanamoorthy S, Minh BQ, Wong TKF, von Haeseler A, Jermiin LS. 2017. ModelFinder: Fast model selection for accurate phylogenetic estimates. *Nature Methods* 14: 587–589.
- Katoh K, Standley DM. 2013. MAFFT multiple sequence alignment software version 7: Improvements in performance and usability. *Molecular Biology and Evolution* 30: 772–780.
- Kearse M, Moir R, Wilson A, Stones-Havas S, Cheung M, Sturrock S, Buxton S, Cooper A, Markowitz S, Duran C *et al.* 2012. Geneious basic: An integrated and extendable desktop software platform for the organization and analysis of sequence data. *Bioinformatics* 28: 1647–1649.
- Kim D, Pertea G, Trapnell C, Pimentel H, Kelley R, Salzberg SL. 2013. TOPHAT2: accurate alignment of transcriptomes in the presence of insertions, deletions and gene fusions. *Genome Biology* 14: R36.
- Knie N, Grewe F, Fischer S, Knoop V. 2016. Reverse U-to-C editing exceeds C-to-U RNA editing in some ferns – a monilophyte-wide comparison of chloroplast and mitochondrial RNA editing suggests independent evolution of the two processes in both organelles. *BMC Evolutionary Biology* 16: 134.
- Knoop V. 2023. C-to-U and U-to-C: RNA editing in plant organelles and beyond. *Journal of Experimental Botany* 74: 2273–2294.
- Kudla J, Igloi GL, Metzlfaff M, Hagemann R, Kössel H. 1992. RNA editing in tobacco chloroplasts leads to the formation of a translatable *psbL* mRNA by a C to U substitution within the initiation codon. *EMBO Journal* 11: 1099–1103.
- Kugita M, Kaneko A, Yamamoto Y, Takeya Y, Matsumoto T, Yoshinaga K. 2003. The complete nucleotide sequence of the hornwort (*Anthoceros formosae*) chloroplast genome: Insight into the earliest land plants. *Nucleic Acids Research* 31: 716–721.
- Kuta E, Ochrya R, Przywara L. 1990. Chromosome studies on Polish bryophytes: V. *Polish Botanical Studies* 1: 127–147.
- Lemieux C, Otis C, Turmel M. 2000. Ancestral chloroplast genome in *Mesostigma viride* reveals an early branch of green plant evolution. *Nature* 403: 649–652.
- Li FW, Nishiyama T, Waller M, Frangedakis E, Keller J, Li Z, Fernandez-Pozo N, Barker MS, Bennett T, Blázquez MA *et al.* 2020. *Anthoceros* genomes illuminate the origin of land plants and the unique biology of hornworts. *Nature Plants* 6: 259–272.
- Li H, Handsaker B, Wysoker A, Fennell T, Ruan J, Homer N, Marth G, Abecasis G, Durbin R, 1000 Genome Project Data Processing Subgroup. 2009. The sequence alignment/map format and SAMTOOLS. *Bioinformatics* 25: 2078–2079.
- Li HT, Yi TS, Gao LM, Ma PF, Zhang T, Yang JB, Gitzendanner MA, Fritsch PW, Cai J, Luo Y *et al.* 2019. Origin of angiosperms and the puzzle of the Jurassic gap. *Nature Plants* 5: 461–470.
- Li YF, Luo L, Liu Y, He Q, Yu NN, Gaowa N, Yi ZQ, Wang JJ, Han W, Peng T *et al.* 2024. The bryophyte phylogeny group: A revised familial classification system based on plastid phylogenomic data. *Journal of Systematics and Evolution* 62: 577–588.
- Lincoln FC. 1930. Calculating waterfowl abundance on the basis of banding returns. *United States, Department of Agriculture, Circular* 118: 1–4.
- Lubna AS, Jan R, Asif S, Bilal S, Khan AL, Kim KM, Lee IJ, AL-Harrasi A. 2024. Plastome diversity and evolution in mosses: insights from structural characterization, comparative genomics, and phylogenetic analysis. *International Journal of Biological Macromolecules* 257: 128608.

- Myers N, Mittermeier RA, Mittermeier CG, da Fonseca GA, Kent J. 2000. Biodiversity hotspots for conservation priorities. *Nature* 6772: 853–858.
- Nguyen LT, Schmidt HA, von Haeseler A, Minh BQ. 2015. IQ-TREE: A fast and effective stochastic algorithm for estimating Maximum-Likelihood phylogenies. *Molecular Biology and Evolution* 32: 268–274.
- Oldenkott B, Yamaguchi K, Tsuji-Tsukinoki S, Knie N, Knoop V. 2014. Chloroplast RNA editing going extreme: more than 3400 events of C-to-U editing in the chloroplast transcriptome of the lycophyte *Selaginella uncinata*. *RNA* 20: 1499–1506.
- Ong HC, Palmer JD. 2006. Pervasive survival of expressed mitochondrial pseudogenes in grasses and their relatives for 80 million years following three functional transfers to the nucleus. *BMC Evolutionary Biology* 6: 55.
- Peñaloza-Bojarcá GF, Burleigh JG, Maciel-Silva A, Cargill DC, Bell D, Sessa EB, McDaniel SF, Davis EC, Endara L, Allen NS *et al.* 2025. Ancient reticulation, incomplete lineage sorting and the evolution of the pyrenoid at the dawn of hornwort diversification. *Annals of Botany* 135: 1199–1213.
- Peñaloza-Bojarcá GF, Sierra AM, Becher H, Renzaglia KS, Villarreal JC. 2022. Historical biogeography of the austral hornwort genus *Phaeomegaceros* (Dendrocerotaceae, Anthocerotophyta). *Bryophyte Diversity and Evolution* 45: 044–066.
- Peng T, Zhu RL. 2014. A revision of the genus *Notothylas* (Notothyladaceae, Anthocerotophyta) in China. *Phytotaxa* 156: 156–164.
- Pollock DD, Zwickl DJ, McGuire JA, Hillis DM. 2002. Increased taxon sampling is advantageous for phylogenetic inference. *Systematic Biology* 51: 664–671.
- Proskauer J. 1957. Studies on Anthocerotales V. *Phytomorphology* 7: 113–135.
- Rabosky DL. 2014. Automatic detection of key innovations, rate shifts, and diversity-dependence on phylogenetic trees. *PLoS ONE* 9: e89543.
- Rabosky DL, Grudler M, Anderson C, Title P, Shi JJ, Brown JW, Huang H, Larson JG. 2014. BAMMtools: an R package for the analysis of evolutionary dynamics on phylogenetic trees. *Methods in Ecology and Evolution* 5: 701–707.
- Ravi V, Khurana JP, Tyagi AK, Khurana P. 2008. An update on chloroplast genomes. *Plant Systematics and Evolution* 271: 101–122.
- Renzaglia KS, Villarreal VC, Duff RJ. 2009. New insights into morphology, anatomy, and systematics of hornworts. In: Goffinet B, Shaw AJ, eds. *Bryophyte biology, 2nd edn*. Cambridge, UK: Cambridge University Press, 139–172.
- Robison TA, Oh ZG, Lafferty D, Xu X, Villarreal JC, Gunn LH, Li FW. 2025. Hornworts reveal a spatial model for pyrenoid-based CO₂-concentrating mechanisms in land plants. *Nature Plants* 11: 63–73.
- Robison TA, Wolf PG. 2019. ReFermment: an R package for annotating RNA editing in plastid genomes. *Applications in Plant Sciences* 7: e01216.
- Ronquist F, Teslenko M, van der Mark P, Ayres DL, Darling A, Höhna S, Larget B, Liu L, Suchard MA, Huelsenbeck JP. 2012. MrBayes 3.2: efficient bayesian phylogenetic inference and model choice across a large model space. *Systematic Biology* 61: 539–542.
- Ruaud S, Nötzold SI, Waller M, Galbier F, Mousavi SS, Charran M, Mateos JM, Zeeman S, Bailly A, Baroux C *et al.* 2025. Molecular underpinnings of hornwort CO₂ concentrating mechanisms: subcellular localization of putative key molecular components in the model hornwort *Anthoceros agrestis*. *New Phytologist* 247: 1244–1262.
- Rüdinger M, Polskiewicz M, Knoop V. 2008. Organellar RNA editing and plant-specific extensions of pentatricopeptide repeat proteins in jungermanniid but not in marchantiid liverworts. *Molecular Biology and Evolution* 25: 1405–1414.
- Sadamitsu A, Inoue Y, Sakakibara K, Tsubota H, Yamaguchi T, Deguchi H, Nishiyama T, Shimamura M. 2021. The complete plastid genome sequence of the enigmatic moss, (Takakiopsida, Bryophyta): evolutionary perspectives on the largest collection of genes in mosses and the intensive RNA editing. *Plant Molecular Biology* 107: 431–449.
- Schafraan P, Hauser DA, Nelson JM, Xu X, Mueller LA, Kulshrestha S, Smalley I, de Vries S, Irisarri I, de Vries J *et al.* 2025. Pan-phylum genomes of hornworts reveal conserved autosomes but dynamic accessory and sex chromosomes. *Nature Plants* 11: 49–62.
- Shen C, Li H, Shu L, Huang WZ, Zhu RL. 2025. Ancient large-scale gene duplications and diversification in bryophytes illuminate the plant terrestrialization. *New Phytologist* 245: 2292–2308.
- Shen C, Xu H, Huang WZ, Zhao Q, Zhu RL. 2024. Is RNA editing truly absent in the complex thalloid liverworts (Marchantiopsida)? Evidence of extensive RNA editing from *Cyathodium cavernarum*. *New Phytologist* 242: 2817–2831.
- Sloan DB. 2017. Nuclear and mitochondrial RNA editing systems have opposite effects on protein diversity. *Biology Letters* 13: 20170314.
- Small ID, Schallenberg-Rüdinger M, Takenaka M, Mireau H, Osterseizer-Biran O. 2020. Plant organellar RNA editing: what 30 years of research has revealed. *The Plant Journal* 101: 1040–1056.
- Smith EC, Griffiths H. 1996. A pyrenoid-based carbon concentrating mechanism is present in terrestrial bryophytes of the class Anthocerotae. *Planta* 200: 203–212.
- Söderström L, Hagborg A, von Konrat M, Bartholomew-Began SE, Bell D, Briscoe L, Brown EA, Cargill DC, Costa DP, Crandall-Stotler BJ *et al.* 2016. World checklist of hornworts and liverworts. *PhytoKeys* 59: 1–828.
- Stech M, Quandt D, Frey W. 2003. Molecular circumscription of the hornworts (Anthocerotophyta) based on the chloroplast DNA *trnL-trnF* region. *Journal of Plant Research* 116: 389–398.
- Sugiura C, Kobayashi Y, Aoki S, Sugita C, Sugita M. 2003. The complete chloroplast DNA sequence of the moss *Physcomitrella patens*. Evidence for the loss and relocation of *rpoA* from the chloroplast to the nucleus. *Nucleic Acids Research* 31: 5324–5331.
- Takenaka M, Zehrmann A, Verbitskiy D, Härtel B, Brennicke A. 2013. RNA editing in plants and its evolution. *Annual Review of Genetics* 47: 335–352.
- Tillich M, Lehwark P, Pellizzer T, Ulbricht-Jones ES, Fischer A, Bock R, Greiner S. 2017. GeSeq – versatile and accurate annotation of organelle genomes. *Nucleic Acids Research* 45: 6–11.
- Tonti-Filippini J, Nevill PG, Dixon K, Small I. 2017. What can we do with 1000 plastid genomes? *The Plant Journal* 90: 808–818.
- Turmel M, Otis C, Lemieux C. 2005. The complete chloroplast DNA sequences of the charophycean green algae and reveal that the chloroplast genome underwent extensive changes during the evolution of the Zygnematales. *BMC Biology* 3: 22.
- Turudić A, Liber Z, Grdiša M, Jakšić J, Varga F, Šatović Z. 2023. Variation in chloroplast genome size: biological phenomena and technological artifacts. *Plants* 12: 254.
- Villarreal JC, Cargill DC, Goffinet B. 2010a. *Phaeomegaceros squamuliger* subspecies *hasselii* (Dendrocerotaceae, Anthocerotophyta), a new taxon from the Southern Hemisphere. *Nova Hedwigia* 91: 349–360.
- Villarreal JC, Cargill DC, Hagborg A, Soderstrom L, Renzaglia KS. 2010b. A synthesis of hornwort diversity: patterns, causes and future work. *Phytotaxa* 9: 150–166.
- Villarreal JC, Cargill DC, Söderström L, Hagborg A, von Konrat M. 2015a. Notes on early land plants today. 70. Nomenclatural notes in hornworts (Anthocerotophyta). *Phytotaxa* 208: 92–96.
- Villarreal JC, Cusimano N, Renner SS. 2015b. Biogeography and diversification rates in hornworts: the limitations of diversification modeling. *Taxon* 64: 229–238.
- Villarreal JC, Forrester LL, Wickett N, Goffinet B. 2013. The plastid genome of the hornwort *Nothoceros aenigmaticus* (Dendrocerotaceae): Phylogenetic signal in inverted repeat, pseudogenization, and intron gain. *American Journal of Botany* 100: 467–477.
- Villarreal JC, Renner SS. 2012. Hornwort pyrenoids, carbon-concentrating structures, evolved and were lost at least five times during the last 100 million years. *Proceedings of the National Academy of Sciences, USA* 109: 18873–18878.
- Villarreal JC, Turmel M, Bourgouin-Couture M, Laroche J, Allen NS, Li FW, Cheng SF, Renzaglia K, Lemieux C. 2018. Genome-wide organellar analyses from the hornwort *Leiosporoceros dussii* show low frequency of RNA editing. *PLoS ONE* 13: e0200491.
- Wickett NJ, Zhang Y, Hansen SK, Roper JM, Kuehl JV, Plock SA, Wolf PG, DePamphilis CW, Boore JL, Goffinet B. 2008. Functional gene losses occur with minimal size reduction in the plastid genome of the parasitic liverwort *Aneura mirabilis*. *Molecular Biology and Evolution* 25: 393–401.
- Wolf PG, Rowe CA, Hasebe M. 2004. High levels of RNA editing in a vascular plant chloroplast. *Gene* 339: 89–97.

- Wolfe KH, Li WH, Sharp PM. 1987. Rates of nucleotide substitution vary greatly among plant mitochondrial, chloroplast, and nuclear DNAs. *Proceedings of the National Academy of Sciences, USA* 84: 9054–9058.
- Xiang YL, Jin XJ, Shen C, Cheng XF, Shu L, Zhu RL. 2022. New insights into the phylogeny of the complex thalloid liverworts (Marchantiopsida) based on chloroplast genomes. *Cladistics* 38: 649–662.
- Yang BY. 1960. Studies on Taiwan Hepaticae. I. A preliminary list of the Hepaticae of Taiwan. *Quarterly Journal of the Taiwan Museum* 13: 231–235.
- Yang ZH. 2007. PAML 4: phylogenetic analysis by maximum likelihood. *Molecular Biology and Evolution* 24: 1586–1591.
- Yu Y, Liu HM, Yang JB, Ma WZ, Pressel S, Wu YH, Schneider H. 2019. Exploring the plastid genome disparity of liverworts. *Journal of Systematics and Evolution* 57: 382–394.
- Zhang J, Fu XX, Li RQ, Zhao X, Liu Y, Li MH, Zwaenepoel A, Ma H, Goffinet B, Guan YL *et al.* 2020. The hornwort genome and early land plant evolution. *Nature Plants* 6: 107–118.
- Zhang L, Zuo Q, Li JY, Peng T. 2018. A new species of *Notothylas* (Notothyladaceae) from Southwest China. *Phytotaxa* 367: 191–195.

Supporting Information

Additional Supporting Information may be found online in the Supporting Information section at the end of the article.

Fig. S1 Information on plastid genomes of various genera in hornworts.

Fig. S2 Comparison of phylogenetic trees based on DNA-ML, DNA-BI, and amino acid-ML.

Fig. S3 Comparison of phylogenetic trees without branch lengths.

Fig. S4 Phylogenetic tree of *Paraphymatoceros* constructed using ML and BI based on *rbcl*, *rps4*, *matK*, and *nad5* sequences.

Fig. S5 Phylogenetic tree of *Phymatoceros* constructed using ML and BI based on *rbcl*, *rps4*, *matK*, and *nad5* sequences.

Fig. S6 The genus-level phylogenetic topologies were inferred from the plastid genome DNA sequences and the transcriptome sequences of plastid PCGs.

Fig. S7 The numbers at each node correspond to node IDs.

Notes S1 Key to species of *Paraphymatoceros* and description of *Paraphymatoceros luguhuensis*.

Notes S2 Key to species of *Phymatoceros* and description of *Phymatoceros verrucosporus*.

Notes S3 An updated classification of hornworts.

Table S1 Comprehensive information on the plastomes of hornworts and outgroups used in the present study.

Table S2 Sequences used in the phylogenetic relationship of *Paraphymatoceros*.

Table S3 Sequences used in the phylogenetic relationship of *Phymatoceros*.

Table S4 Sampling fraction used in BAMM analysis of each genus in hornworts.

Table S5 The details of RNA editing sites in *Dendroceros* sp. 2 Thailand.

Table S6 The details of RNA editing sites in *Notothylas* cf. *guizhouensis* China.

Table S7 The details of RNA editing sites in *Paraphymatoceros luguhuensis* China II.

Table S8 The details of RNA editing sites in *Phaeoceros carolinianus* China V.

Table S9 The details of RNA editing sites in *Phymatoceros bulbiculosus* China I.

Table S10 Predicted, transcriptome-identified, overlapping, and estimated total RNA editing sites based on abnormal start and stop codons.

Table S11 The divergence dates of genera obtained by MCMCTree.

Table S12 Posterior time for each node inferred from MCMCTree with mean and 95% CI age.

Table S13 The sizes and GC contents of the PCGs, tRNA, rRNA, and noncoding regions for representative taxa of charophytes, chlorophytes, liverworts, mosses, lycophytes, ferns, gymnosperms, and angiosperms.

Please note: Wiley is not responsible for the content or functionality of any Supporting Information supplied by the authors. Any queries (other than missing material) should be directed to the *New Phytologist* Central Office.

Disclaimer: The New Phytologist Foundation remains neutral with regard to jurisdictional claims in maps and in any institutional affiliations.